

Assignment

Research Paper Title:***Modelling of Tool Wear in Ultrasonic Vibration Assisted Milling of Ti-6Al-4V***

Inv.- Nr.: 2018/40200
Author: Alpcan Güray
Date of Issue: 16.11.2017

Supervisor: Philipp Rinck
Submission: 15.05.2018

Initial Situation:

Since Taylor introduced the well-known Taylor equation much has changed in the machining industry. Nowadays there is a growing interest on hybrid machining processes like ultrasonic vibration assisted machining to achieve extended tool life, better surface qualities, to reduce cutting forces and to suppress burr formation. Tool wear is affected by various complex factors like mechanical, chemical and physical properties of tool and workpiece materials. A better understanding of the effects of ultrasonic vibrations on tool wear is needed to schedule tool changes and achieve consistent surface qualities.

Titanium's low density, high strength and high corrosion resistance makes titanium the material of choice for reliable lightweight products. However, titanium and its alloys are well known for being hard to machine materials as the low thermal conductivity causes high temperatures at the cutting edge, combined with the high chemical reactivity with commonly used tool materials, causes tools to wear at much higher rates.

Objective Targets:

Main goal of this thesis is to develop a model, that would be able to describe tool wear in ultrasonic vibration assisted milling of Ti-6Al-4V. Scenarios such as vibration assisted milling with periodic tool-workpiece contact and without periodic tool-workpiece contact must be modelled. Existing tool life models must be researched and dominant tool wear mechanisms of Ti-6Al-4V must be discussed to develop an accurate tool life model.

Methodology:

- Researching and understanding dominant wear mechanisms in Titanium machining
- Literature review of existing tool wear models
- Choosing a tool wear model that is able to describe dominant wear mechanisms of Ti-6Al-4V milling
- Extending the chosen tool wear model for ultrasonic vibration assisted milling
- Experimental validation of the developed tool wear model

Agreement:

This work includes intellectual property of the *iwb*, as B.Sc. Alpcan Güray is supervised by Dipl.-Ing. Philipp Rinck. A publication or disclosure of the work to third parties requires the approval of the chair holder. I agree to the archival storage of my thesis in the *iwb* library, which is owned by the *iwb* and only accessible to its staff members. I also agree to the contribution of this work to the digital thesis database of the *iwb* in the form of a PDF-document.

Munich, 15.05.2018

Prof. Dr.-Ing. Michael Zäh

Dipl.-Ing. Philipp Rinck

B.Sc. Alpcan Güray

Table of Contents

| | | |
|-------|---|-----|
| I | Abstract | iii |
| II | List of Figures | iv |
| III | List of Tables | v |
| IV | Nomenclature | vi |
| V | Acknowledgement | xi |
| 1 | Introduction | 1 |
| 1.1 | Motivation..... | 1 |
| 1.2 | Aims | 2 |
| 1.3 | Outline..... | 2 |
| 2 | Background | 3 |
| 2.1 | Ti-6Al-4V | 3 |
| 2.1.1 | Chemical Properties | 4 |
| 2.1.2 | Physical and Mechanical Properties | 4 |
| 2.2 | Milling Process | 5 |
| 2.2.1 | Conventional Milling..... | 5 |
| 2.2.2 | Ultrasonic Vibration Assisted Milling | 6 |
| 2.3 | Wear Mechanisms..... | 7 |
| 2.3.1 | Abrasive Wear | 7 |
| 2.3.2 | Adhesive Wear | 8 |
| 2.3.3 | Diffusion Wear | 8 |
| 2.3.4 | Chemical Wear..... | 9 |
| 2.3.5 | Wear due to Plastic Deformation | 9 |
| 2.4 | Cutting Tool Wear | 10 |
| 2.4.1 | Crater Wear | 11 |
| 2.4.2 | Flank Wear | 11 |
| 2.4.3 | Chipping | 12 |
| 2.4.4 | Fracture | 12 |
| 2.4.5 | Notch Wear..... | 13 |
| 2.4.6 | Coating Delamination..... | 13 |
| 2.4.7 | Chatter..... | 13 |
| 2.5 | Modelling and Prediction of Tool Life..... | 14 |
| 2.5.1 | Taylor-Type Equations..... | 14 |
| 2.5.2 | Equations Based on Chip-Equivalent Concept..... | 15 |

| | | |
|----------|---|-----------|
| 2.5.3 | Equations Depending on Pressure and Hardness..... | 17 |
| 2.5.4 | Equations Depending on Temperature | 18 |
| 2.5.5 | Other Models | 19 |
| 3 | Modelling of Tool Wear in Ultrasonic Vibration Assisted Milling | 20 |
| 3.1 | Choosing the Tool Life Model | 20 |
| 3.2 | Extending the Tool Life Model for Ultrasonic Vibration Assisted Milling | 22 |
| 3.2.1 | Modelling the Maximum Equivalent Chip Thickness in Milling..... | 22 |
| 3.2.2 | Modelling the Phase With Periodic Tool and Workpiece Separation | 27 |
| 3.2.3 | Modelling the Phase Without Tool and Workpiece Separation..... | 33 |
| 4 | Experimental Validation | 37 |
| 4.1 | Experimental Equipment and Setting..... | 37 |
| 4.2 | Tool Wear Experiments..... | 39 |
| 5 | Summary and Future Work | 44 |
| 6 | Bibliography..... | 46 |
| 7 | Content of the CD | 56 |
| 8 | Statutory Declaration..... | 57 |

I Abstract

Titanium's low density, high strength and high corrosion resistance makes titanium the material of choice for reliable lightweight products. Nowadays there is a growing interest on hybrid machining processes like ultrasonic vibration assisted machining to achieve extended tool life, better surface qualities, to reduce cutting forces and to suppress burr formation.

This work investigates the effects of ultrasonic vibration assisted milling on tool wear and presents two equivalent chip thickness based models, that would be able to describe tool life in ultrasonic vibration assisted milling with and without periodic tool-workpiece separation. In this work existing tool wear models for conventional milling are found and grouped, a method for calculating undeformed chip thickness in milling is presented. Dominant wear mechanisms and tool failure modes that occur during machining of commonly used titanium alloy Ti-6Al-4V are discussed. Tool wear experiments showed 13% less tool wear when ultrasonic vibration assistance was introduced.

II List of Figures

- Figure 2-1: Movements in vertical milling process (WAN ET AL. 2017).....
- Figure 2-2: Vibration directions in ultrasonic vibration assisted milling according to CONG & PEI (2013).....
- Figure 2-3: Typical hot hardness characteristics of some tool materials (HOSSEINI & KISHAWY 2014).....
- Figure 2-4: Wear map for rough milling of Ti-6Al-4V with carbide tools according to OOSTHUIZEN (2010).....
- Figure 2-5: Crater wear and measurement ISO 3685:1993.....
- Figure 2-6: Flank wear, notch wear and measurement based on ISO 3685:1993.....
- Figure 3-1: Varying undeformed chip thickness for a slotting operation.....
- Figure 3-2: Torsional and longitudinal ultrasonic vibration assisted face milling
- Figure 3-3: Slotting with carbide milling cutter (left), Visualization of tool workpiece separation during longitudinal vibration assisted milling (right).....
- Figure 3-4: Influence of helix angle to contact time according to BIGELMAIER (2017).....
- Figure 3-5: Theoretical amounts of tool wear during ultrasonic vibration assisted milling....
- Figure 4-1: Longitudinal vibration measurement setup (left) and parts of the main spindle (right).....
- Figure 4-2: Illustration of HPTM solid carbide tool.....
- Figure 4-3: New carbide tool side view (left) and top view (right).....
- Figure 4-4: End cutting edge of 1st flute of the tool after 14,4 m of conventional milling (left) and vibration assisted milling (right).....
- Figure 4-5: Relief flank wear on the 4th flute after 12,6 minutes (14,4 m) of conventional milling (left) and vibration assisted milling (right).....
- Figure 4-6: Relief side of the 3rd flute after 28 minutes (14,4m) of conventional milling (left) and vibration assisted milling (right).....

III List of Tables

Table 2-1: Chemical composition of Ti-6Al-4V in weight percent according to (UHLIG 2018)

Table 2-2: Physical and mechanical Properties of Ti-6Al-4V according to AZO MATERIALS
(2002).....

Table 4-1: Tool dimensions.....

Table 4-2: Experimental conditions for tool life testing.....

IV Nomenclature

Acronyms

| | |
|------|---------------------------------------|
| CM | Conventional milling |
| UVAM | Ultrasonic vibration assisted milling |

Greek Symbols

| | | |
|-------------------|-------------------------|--|
| α | <i>rad</i> | Current end cutting edge position angle |
| α | — | Experimentally determined tool life constant |
| α_q | — | A constant depending on q |
| β | — | Experimentally determined tool life constant |
| β | <i>rad</i> | Helix angle of the carbide cutter |
| γ | — | Experimentally determined tool life constant |
| $\Delta x_{os,l}$ | <i>mm</i> | Distance between the recently cut surface and the rake face of the tool caused by longitudinal oscillation |
| $\Delta x_{os,t}$ | <i>mm</i> | Distance between the recently cut surface and the rake face of the tool caused by torsional oscillation |
| δ | — | Experimentally determined tool life constant |
| Θ | <i>K</i> | Local temperature |
| σ_a | <i>N/mm²</i> | Abrasive wear resistance of tool material |
| σ_t | <i>N/mm²</i> | Normal stresses on the contact surface |
| K | <i>rad</i> | Major cutting angle |
| φ_s | <i>rad</i> | Wrap angle |

Latin Symbols

| | | |
|-----------|----------------------|--|
| a | — | Experimentally determined tool life constant |
| a_e | mm | Radial depth of cut |
| a_p | mm | Axial depth of cut |
| A | mm ² | Actual area of cut |
| A_A | s ⁻¹ | Frequency factor of Arrhenius equation |
| A_c | mm ² | Characteristic cross-sectional area of cut |
| A_l | μm | Amplitude of longitudinal vibration |
| $A_{l,z}$ | μm | Movement of a fixed point on the tool in axial direction |
| A_{Max} | mm ² | Maximum area of cut |
| A_{os} | μm | Oscillation amplitude |
| A_t | μm | Amplitude of torsional vibration |
| A_{TM} | mm ³ /m | Material specific constant for tool life equation of Takeyama and Murata |
| b | — | Experimentally determined tool life constant |
| B_{TM} | mm ³ /min | Material specific constant for tool life equation of Takeyama and Murata |
| c | — | Experimentally determined tool life constant |
| c_b | moles/mole | Concentration of carbon of carbon at the reaction layer/chip boundary |
| c_o | moles/mole | Concentration of carbon of carbon at the reaction layer/tool boundary |
| c_t | moles/mole | Concentration of carbon of carbon in the tool material |
| C | — | Experimentally determined tool life constant |
| C_1 | — | Experimentally determined tool life constant |
| C_2 | — | Experimentally determined tool life constant |
| C_T | — | Taylor constant |
| C_{TM} | J/mol · K | Material specific constant for tool life equation of Takeyama and Murata |
| d | — | Experimentally determined tool life constant |

| | | |
|--------------|---------------------|---|
| D_c | cm^2/sec | Diffusion coefficient of carbon in the titanium carbide reaction layer |
| D | mm | Tool diameter |
| e | — | Experimentally determined tool life constant |
| E_a | J/mol | Activation energy |
| f | — | Experimentally determined tool life constant |
| f | mm/min | Feed rate |
| f_{os} | Hz | Oscillation frequency |
| f_r | mm | Feed per revolution |
| f_z | $mm/tooth$ | Feed rate per tooth |
| g | — | Experimentally determined tool life constant |
| g_0 | — | A constant equal or greater than 0 |
| g_1 | — | Experimentally determined constant |
| G_* | — | A tool and workpiece specific constant, which refers to the tool life T_* |
| h | — | Experimentally determined tool life constant |
| h_e | mm | Characteristic depth of cut |
| h_e | mm | Equivalent chip thickness |
| $h_{eq,Max}$ | mm | Maximum equivalent chip thickness |
| h_m | mm | Average chip thickness |
| h_{ud} | mm | Undeformed chip thickness |
| $h_{ud,Max}$ | mm | Maximum undeformed chip thickness |
| H | $mm^3 \cdot s^2/kg$ | Hardness of the softer material |
| H_i | $mm^3 \cdot s^2/kg$ | Hardness of the surface asperities |
| i_s | — | Slope of the $\log(T)$ - $\log(f_z)$ plot |
| i_f | — | Experimentally determined tool life constant for Depiereux equation |
| k | — | Experimentally determined tool life constant |

| | | |
|-----------|---|---|
| k_s | — | Slope of the log(T)-log(v_c) plot |
| k_v | — | Experimentally determined tool life constant for Depiereux equation |
| K | — | Probability of removing a wear particle per unit distance travel |
| L | mm | Length of the engaged cutting edge |
| L_c | mm | Cutting distance |
| L_{Max} | mm | Maximum length of the engaged cutting edge |
| L_s | mm | Sliding distance |
| m_d | — | Experimentally determined tool life constant for Depiereux equation |
| m_f | mm ⁻¹ | Milling equivalent of Colding |
| n | rpm | Spindle speed |
| n_d | — | Experimentally determined tool life constant for Depiereux equation |
| N | N | Normal Force |
| p | N · mm ² | Pressure |
| q | 1/mm | Chip equivalent |
| q_0 | — | A simple function of T |
| r | mm | Tool radius |
| r_e | mm | Tool nose radius |
| R | J · K ⁻¹ · mol ⁻¹ | Universal gas constant |
| s | mm | Sliding distance |
| t | cm | Thickness of the titanium carbide reaction layer |
| t | s | Time |
| t_c | min | Cutting time |
| t_c | s | Contact time during an oscillation cycle |
| t_{e1} | s | Tool entry time |
| t_{e2} | s | Tool exit time |

| | | |
|----------------|-----------------------|---|
| t_p | s | Oscillation cycle duration |
| t_{nc} | s | Time passed without a contact during an oscillation cycle |
| T | min | Tool life |
| T_* | min | A certain tool life |
| T_c | — | Contact ratio |
| v_c | m/min | Cutting speed |
| v_{os} | m/min | Oscillation speed |
| $v_{os,crit}$ | m/min | Critical oscillation speed required to cause tool-workpiece separation |
| $v_{os,l}$ | m/min | Oscillation speed in cutting direction caused by longitudinal vibration |
| $v_{os,l,Max}$ | m/min | Maximum oscillation speed in cutting direction caused by longitudinal vibration |
| $v_{os,Max}$ | m/min | Maximum oscillation speed |
| $v_{UV,co}$ | m/min | Combined torsional and longitudinal vibration speed |
| v_{UV} | m/min | Resulting torsional and longitudinal vibration speed in cutting direction |
| V_b | cm ³ /mole | Molar volume of the reaction layer/chip boundary |
| V_o | cm ³ /mole | Molar volume of the reaction layer/tool boundary |
| V_t | cm ³ /mole | Molar volume of the tool material |
| W | mm ³ | Wear volume |
| W_a | mm ³ | Mechanical wear volume |
| W_r | mm ³ | Physicochemical wear volume |
| z | — | Number of flutes |
| Z | — | Atomic layers of the imagined coherent film |

V Acknowledgement

1 Introduction

Since TAYLOR (1907) introduced the well-known Taylor equation much has changed in the machining industry. Nowadays there is a growing interest on hybrid machining processes like ultrasonic vibration assisted machining to achieve extended tool life, better surface qualities, to reduce cutting forces and to suppress burr formation (BREHL & DOW 2008). Tool wear is affected by various complex factors like mechanical, chemical and physical properties of tool and workpiece materials. A better understanding of the effects of ultrasonic vibrations on tool wear is needed to schedule tool changes and achieve consistent surface qualities.

Titanium's low density, high strength and high corrosion resistance makes titanium the material of choice for reliable lightweight products. However, titanium and its alloys are well known for being hard to machine materials as the low thermal conductivity causes high temperatures at the cutting edge, combined with the high chemical reactivity with commonly used tool materials, causes tools to wear at much higher rates.

1.1 Motivation

The growing demand on superalloys such as nickel and titanium alloys need new advanced machining technologies to match the required production rates. Such a technology was introduced in 1960's by superimposing high frequency ultrasonic vibrations on the conventional movement of the cutting tool (BABITSKY ET AL. 2003).

Most of the researches conducted about vibration assisted machining, were about turning and grinding, much less attention was given for ultrasonic vibration assisted milling due to the complex trajectory of the tool tip and the periodically changing chip thickness (ZHANG ET AL. 2017).

When compared with conventional machining ultrasonic vibration assisted machining has many benefits. PUJANA ET AL. (2009) conducted ultrasonic vibration assisted drilling experiments on Ti-6Al-4V and observed 10-20% less feed forces. JANGHORBANIAN ET AL. (2013) conducted ultrasonic vibration assisted milling experiments on austenitic stainless steel AISI 304 and observed that an increase on vibration amplitude decreased the cutting forces.

TSAI ET AL. (2016) observed less tool wear during longitudinal ultrasonic vibration assisted milling of hard mold steel, similar results were also found by LI ET AL. (2012). Although there has been quite a lot of research about tool wear in ultrasonic vibration assisted machining no tool wear models were developed so far.

1.2 Aims

Main goal of this thesis is to develop a model, that would be able to describe tool wear in ultrasonic vibration assisted milling of Ti-6Al-4V. To achieve the main goal of the thesis following subgoals are needed to be achieved:

- Researching and understanding dominant wear mechanisms in Titanium machining
- Literature review of existing tool wear models
- Choosing a tool wear model that is able to describe dominant wear mechanisms of Ti-6Al-4V milling
- Extending the chosen tool wear model for ultrasonic vibration assisted milling
- Experimental validation of the developed tool wear model

1.3 Outline

In this thesis, a new tool life model is presented, that will be able to describe tool wear in ultrasonic vibration assisted milling of Ti-6Al-4V.

In Chapter 2 the essential background information for understanding tool wear will be given. The physical and chemical properties of Ti-6Al-4V is investigated to understand the dominant tool wear mechanisms during milling. The differences between conventional and ultrasonic vibration assisted milling are researched in the literature to find out the effects of ultrasonic vibrations on tool wear. Existing tool life models are researched, effects and assumptions made for the models are discussed.

In Chapter 3 an existing tool life model is chosen for further development to describe the tool life in ultrasonic vibration assisted milling of Ti-6Al-4V. In order to model the effects of ultrasonic vibrations, vibration assisted milling is separated into two scenarios due to ultrasonic vibrations; the first with periodic tool-workpiece separation and the second one without periodic tool-workpiece separation.

The experimental validation of the developed models are done in Chapter 4. At first the experimental equipment and the tool wear test setup is presented. The tool wear patterns will be discussed for both conventional and ultrasonic vibration assisted milling of Ti-6Al-4V.

Finally, the presented tool life model for ultrasonic vibration assisted milling is summarized and evaluated in Chapter 5. Possible points for future research fields of tool wear and ultrasonic vibration assisted milling are given.

2 Background

This chapter provides necessary information and the theoretical background to understand following parts of the thesis. To begin with we will investigate the physical and chemical properties of Titanium and its alloy Ti-6Al-4V to understand the hard to machine background of the respective materials.

In section two, the conventional and ultrasonic assisted milling will be discussed to understand the basic parameters of conventional milling and the effects of ultrasonic vibrations.

In section three, wear mechanisms such as; abrasive, adhesive, diffusion and chemical wear and wear due to plastic deformation, which are significant to cutting tool and that occur during conventional and ultrasonic vibration assisted milling of Ti-6Al-4V, will be discussed.

In the fourth section, the visual appearance of different forms of cutting tool wear and the mechanisms responsible for the wear will be discussed.

Section five will be the modelling and prediction of tool wear. Important tool life prediction models will be grouped and assumptions will be discussed.

2.1 Ti-6Al-4V

Titanium is a transition metal with symbol Ti and atomic number 22. It is a silvery gleaming light metal with high strength and high toughness. In its pure and unalloyed state at room temperature titanium has a hexagonal crystal structure, which is also called α -form. At 882 °C the hexagonal α -form changes into a body-centered cubic lattice. This is a so called β -form and it is softer and more ductile than the α -form. (BARGEL ET AL. 2008, p. 301–304)

Ti-6Al-4V, also called as Grade 5 titanium is a heat treatable $\alpha+\beta$ titanium alloy featuring high strength to weight ratio and high corrosion resistance. According to SUPRA ALLOYS (2018), Ti-6Al-4V is the most commonly used titanium alloy and is applied in wide range of applications, where low density and high corrosion resistance are necessary such as e.g. aerospace industry and marine applications. Because of the low thermal conductivity and high chemical reactivity with many cutting tool materials, titanium alloys are considered as difficult to machine materials (CHE-HARON 2001).

Fehler! Verwenden Sie die Registerkarte 'Start', um Heading 1 dem Text zuzuweisen, der hier angezeigt werden soll.

2.1.1 Chemical Properties

Ti-6Al-4V is composed of both α -form stabilizing aluminum and β -form stabilizing vanadium. The chemical composition of Ti-6Al-4V is given in the following table:

Table 2-1: Chemical composition of Ti-6Al-4V in weight percent according to UHLIG (2018)

| | Al | C | Fe | H | N | O | V | Ti | Remainder Each | Remainder Total |
|------------|------|------|------|-------|------|------|------|---------|-------------------|--------------------|
| Min | 5,50 | -- | -- | -- | -- | -- | 3,50 | -- | -- | -- |
| Max | 6,75 | 0,08 | 0,30 | 0,015 | 0,05 | 0,20 | 4,50 | Balance | 0,10 | 0,40 |

2.1.2 Physical and Mechanical Properties

While desired mechanical properties of Ti-6Al-4V could be obtained by heat treatments, typical property ranges for well-processed Ti-6Al-4V are given in the following table:

Table 2-2: Physical and mechanical Properties of Ti-6Al-4V according to AZO MATERIALS (2002)

| | Units (S.I.) | Minimum Value | Maximum Value |
|---|--|---------------|---------------|
| Density ρ | [g·cm ⁻³] | 4,429 | 4,512 |
| Young's Modulus E | [GPa] | 110 | 119 |
| Poisson's Ratio ν | [\cdot] | 0,31 | 0,37 |
| Ultimate Tensile Strength R_m | [MPa] | 862 | 1200 |
| Yield Strength σ_y | [MPa] | 786 | 910 |
| Melting Point T_m | [°K] | 1605 | 1660 |
| Thermal Expansion α_T | [K ⁻¹] | 8,7 | 9,1 |
| Thermal Conductivity λ | [W·m ⁻¹ · K ⁻¹] | 7,1 | 7,3 |

Machining titanium is characterized with high tool-chip interface temperatures because of the high strength of the material that generates heat during plastic deformation. The high temperatures might cause titanium to ignite and the Young's modulus of elasticity can cause chatter, deflection and rubbing problems during machining. (MACHADO & WALLBANK 2016)

2.2 Milling Process

Milling is the machining process of using rotary cutters with one or more flutes to remove material from a workpiece. During a milling process the milling cutter repeatedly cuts into and exits the working material, which produces varying but periodic chip thickness. According to MÜLLER (1982, p. 19) interrupted cutting during the milling process causes alternating mechanical and thermal stresses of the cutter and the milling machine.

As this thesis deals with modelling tool wear in ultrasonic vibration assisted milling, some basic milling parameters and equations will be introduced in this chapter.

2.2.1 Conventional Milling

As it is seen in Figure 2-1, there are 2 main movements in conventional milling. The first one is the rotational movement of the spindle Ω , which turns with the connected milling cutter that separates chips from the workpiece. The second one depends on the type of the mill, it is either at a certain direction, the movement of the cutter feeding into the workpiece or the workpiece feeding into the cutter, so that in each turn of the milling cutter new workpiece material get in contact.

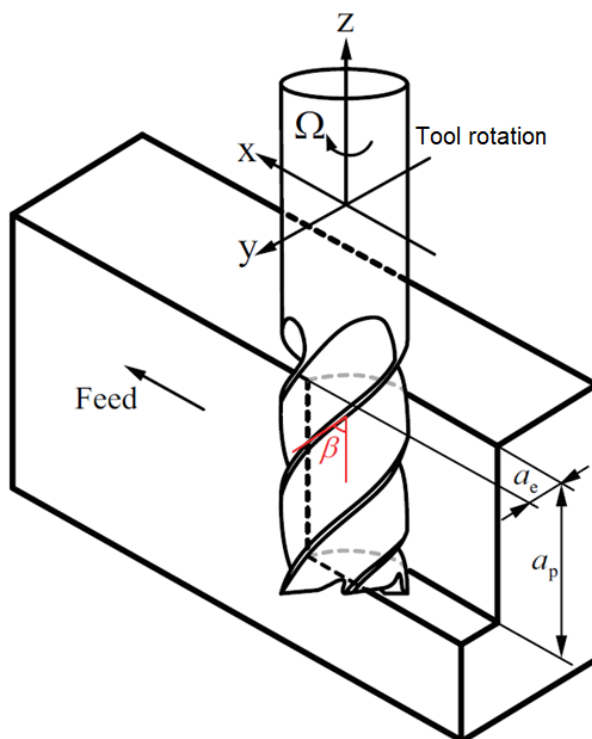


Figure 2-1: Movements in vertical milling process (WAN ET AL. 2017)

The cutting speed v_c and feed rate f are the most important parameters during a milling operation and both depend on the spindle speed n in revolutions per minute (rpm). The cutting speed v_c in m/min, is a function of tool diameter D in mm as shown in Equation 2-1. (ALTINTAS 2011)

$$v_c = \pi \cdot D \cdot n \quad (2-1)$$

The feed rate f in mm/min is a function of the feed rate per tooth f_z in mm and number of flutes z as shown in Equation 2-2. (ALTINTAS 2011)

$$f = f_z \cdot n \cdot z \quad (2-2)$$

An important parameter for wear modelling is the average chip thickness. According to NEE (2013, p. 401) average chip thickness h_m in mm is a function of the feed rate per tooth f_z in mm, tool diameter D in mm, major cutting angle K , wrap angle φ_s and cut width a_e in mm as shown in Equation 2-3.

$$h_m = \frac{360^\circ}{\pi \cdot \varphi_s} \cdot \frac{a_e}{D} \cdot \sin(K) \cdot f_z \quad (2-3)$$

2.2.2 Ultrasonic Vibration Assisted Milling

Ultrasonic vibration assisted milling adds high frequency low amplitude vibrations to the rotary cutter of a conventional milling machine or to the workpiece as seen in Figure 2-2. According to BREHL & Dow (2008) the movement caused by vibration can be seen as a small reciprocating motion (1 dimensional vibration assisted machining) or an elliptical motion (2 dimensional vibration assisted machining) whose centroid moves in the direction of cutting speed. The 2 dimensional elliptical motion is achieved by overlapping vibrations in normal (vertical) and feeding (horizontal) directions which follow linear vibratory tool paths. The vibration directions can be seen in Figure 2-2.

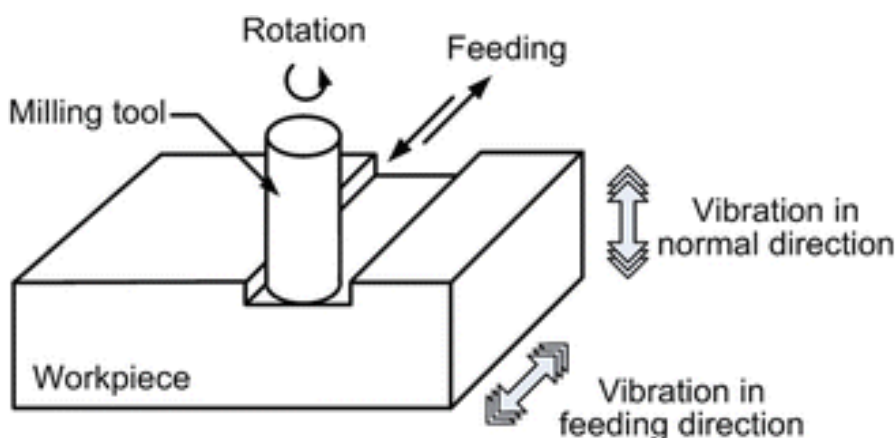


Figure 2-2: Vibration directions in ultrasonic vibration assisted milling according to CONG & PEI (2013)

Ultrasonic vibration assisted machining has many benefits compared to conventional machining methods. According to BREHL & DOW (2008), "2 dimensional vibration assisted machining generally provides longer tool life than 1 dimensional vibration assisted machining for the same depth of cut, tool geometry, and tool-workpiece material combination". Ultrasonic vibration assisted drilling of Ti-6Al-4V compared to conventional drilling shows 20% feed force reduction and zero burr formation (PUJANA ET AL. 2009). While ultrasonic vibration assisted turning of Ti-6Al-4V at cutting speeds higher than 20 m/min , PATIL ET AL. (2014) observed lower temperatures then conventional turning.

Some researchers recorded higher temperatures during experiments. According to BABITSKY ET AL. (2003), ultrasonic vibration assisted turning of Inconel 718 increased temperature of the chip and the cutting edge dramatically, 50% higher temperature was observed . Also PUJANA ET AL. (2009) recorded temperatures near 800°K in conventional drilling of Ti-6Al-4V, but the temperatures were close to 1100°K when he was experimenting with ultrasonic vibration assisted drilling. Titanium has a high strength at elevated temperatures however, higher temperatures can cause thermal softening of the tool tip and cause plastic deformation.

2.3 Wear Mechanisms

During machining operations several wear mechanisms may play a role simultaneously, or one of them may dominate the process by causing cutting tool wear. The main wear mechanisms change with different tool-workpiece combinations.

According to DEARNLEY & GREARSON (2013), diffusion wear dominates the wear on the rake face when machining titanium alloys with uncoated cemented carbide or ceramic (except sialon) tools. However machining experiments done with cubic boron nitride and polycrystalline diamond tools show that diffusion and adhesion are the main wear mechanisms when milling titanium alloys (NABHANI 2001).

The important wear mechanisms that are brought into play when machining Ti-6Al-4V will be introduced in this chapter.

2.3.1 Abrasive Wear

Abrasion happens when a harder material shears away small particles from the softer material. Tool and workpiece materials contain various hard microstructures like carbides, oxides and nitrides, which then get caught between the tool and the workpiece and cause abrasion wear during machining. (ALTINTAS 2011)

2.3.2 Adhesive Wear

Adhesion is the welding of the softer workpiece material to the harder tool surface, which happens when there is relative motion between tool and workpiece under high pressure. The adhered workpiece material is unstable, and when it separates from the cutting tool it tears away small fragments of the tool material causing adhesive wear. (ALTINTAS 2011)

NABHANI (2001) did some turning experiments with a TA-48 $\alpha+\beta$ titanium alloy and identified a critical temperature for each tool material used. It is observed that in higher temperatures adherent surface layers may be formed on the rake face. The critical temperature is 900°C for cubic boron nitride, 760°C for polycrystalline diamond and 740°C for coated carbide tools(TiC/TiC-N/TiN with nitride as the outermost surface layer) when cutting TA-48 titanium alloy. According to KÖNIG ET AL. (1991), adhesion occurs when the coating begins to wear out (coating delamination).

2.3.3 Diffusion Wear

According to CRANK (1979) diffusion is the process by which matter is transported from a region of high concentration to another region of low concentration as a result of a random molecular motion.

During milling processes the temperatures of the tool and the workpiece increase at contact zones, making the atoms at both materials restive which then migrate to the opposite material where the concentration of the same atom is lower. The tool material diffusing to the chip leads to a weakened cutting edge which eventually causes chipping or breakage of the tool. (ALTINTAS 2011)

JAWAID ET AL. (2000) did some face milling experiments and found out that even with the lowest cutting speed: 55m/min and feed: 0.1mm per tooth, diffusion between the coated carbide tool and Ti-6Al-4V workpiece took place. According to MIN & YOUNG (2013) wear by mechanical action (abrasion, adhesion, plastic deformation) can be accelerated by diffusion processes. ZOYA & KRISHNAMURTHY (2000) did some turning experiments with an $\alpha+\beta$ titanium alloy and noted that 700°C could be a critical temperature for the machining of titanium alloys with a cubic boron nitride tool without diffusion processes. Researchers report that during machining titanium alloys under moderate conditions, tool chip interface temperatures can be above 800°C (SU ET AL. 2006).

2.3.4 Chemical Wear

Chemical wear is the general term for the reaction that happens between the cutting tool, workpiece material and surrounding air that contains various elements including oxygen. It is considered as a thermally activated process. (OOSTHUIZEN 2010)

Oxidation is a chemical wear process and can be described according to ALTINTAS (2011), "The atoms in the cutting tool and/or the work material form new molecules at the contact boundary where the area is exposed to the air.".

When machining titanium alloys, most of the potential tool materials either rapidly dissolve in or chemically react with titanium. When machining with polycrystalline diamond or tungsten carbide tools, a stable layer forms between the tool and the chip as result of chemical reactions. This stable adherent layer on the tool surface limits the diffusion and serves for a reduced tool wear rate. (HARTUNG ET AL. 1982)

2.3.5 Wear due to Plastic Deformation

According to EZUGWU ET AL. (2003), plastic deformation and subsequent tool failure occur at cutting speeds over 45m/min while machining titanium alloys with carbide tools because of high temperatures and shear stresses produced by the sliding chip. A detailed hot hardness characteristics of commonly used tool materials is shown in Figure 2-3.

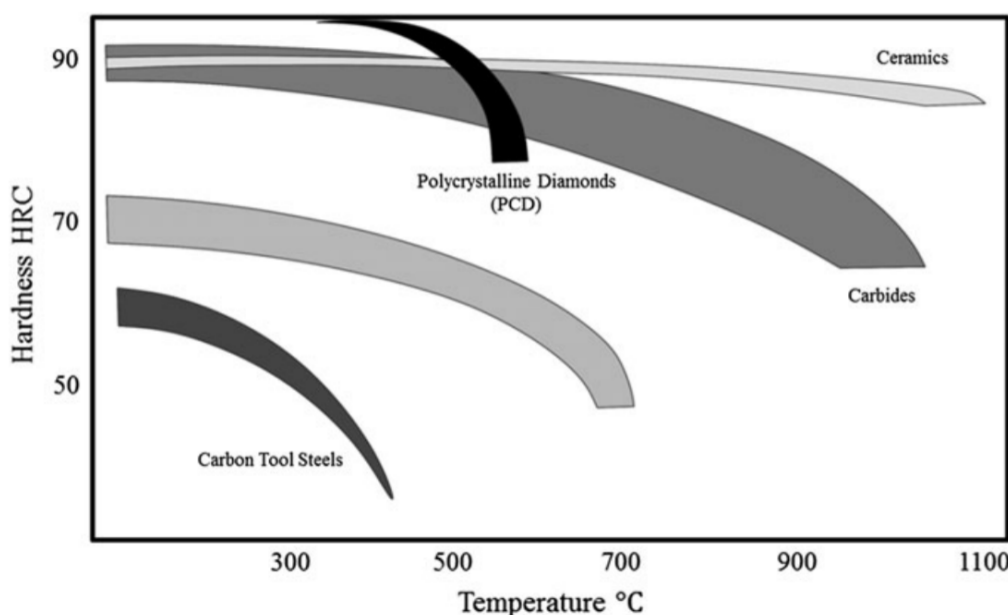


Figure 2-3: Typical hot hardness characteristics of some tool materials (HOSSEINI & KISHAWY 2014)

2.4 Cutting Tool Wear

According to DADIC (2013), tool wear is the “(...)gradual loss of the tool material and change of tools shape during the cutting process which changes cutting properties of the tool”.

There are possible modes by which a cutting tool can wear out and fail. In order to calculate tool wear and schedule tool replacements one should expect degradation (gradual wear). However, tool can fail in a premature, catastrophic way which is the least desirable failure mode, because of its unpredictability. In figure 2-4 tool wear map for the rough milling of Ti-6Al-4V with carbide tools is illustrated depending on maximum un-deformed chip thickness (h_{eMax}) and cutting speed (v_c). (OOSTHUIZEN 2010)

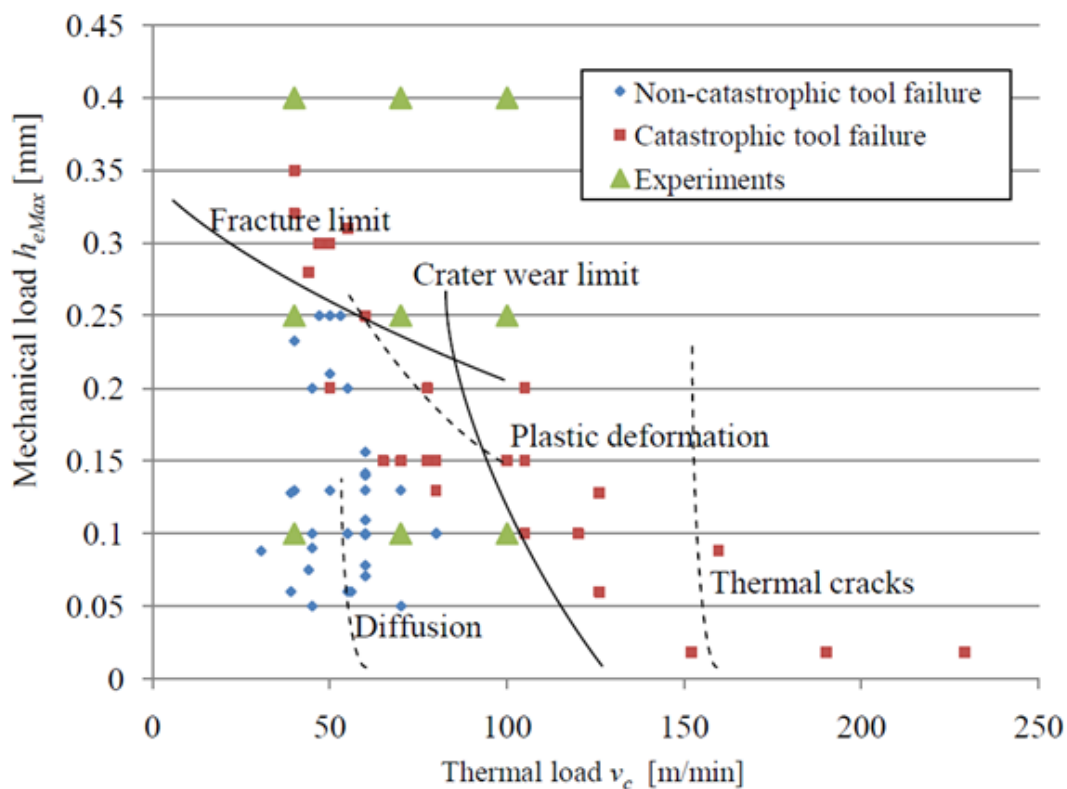


Figure 2-4: Wear map for rough milling of Ti-6Al-4V with carbide tools according to OOSTHUIZEN (2010)

The main wear mechanisms when milling Ti-6Al-4V were explained in chapter 2.3, in the following sections these mechanisms will be linked up to the main cutting tool wear appearances.

2.4.1 Crater Wear

Crater wear is formed on the rake face, and it is caused by the friction force of the moving chip under heavy loads and high temperatures. The temperatures are the greatest near the crater center because of the intensive diffusion caused by the high temperature. Crater wear can be minimized by selecting cutting tools that have low chemical affinity with the work material or use cooling lubricant that penetrates between the chip and tool, lowering friction and cooling down the tool. Thus, reducing the diffusion of the tool material into the chip. (ALTINTAS 2011)

The measured length on a typical crater wear pattern are crater depth (KT), crater width (KB), crater center distance (KM) and crater front distance (KF) as it can be seen in Figure 2-5.

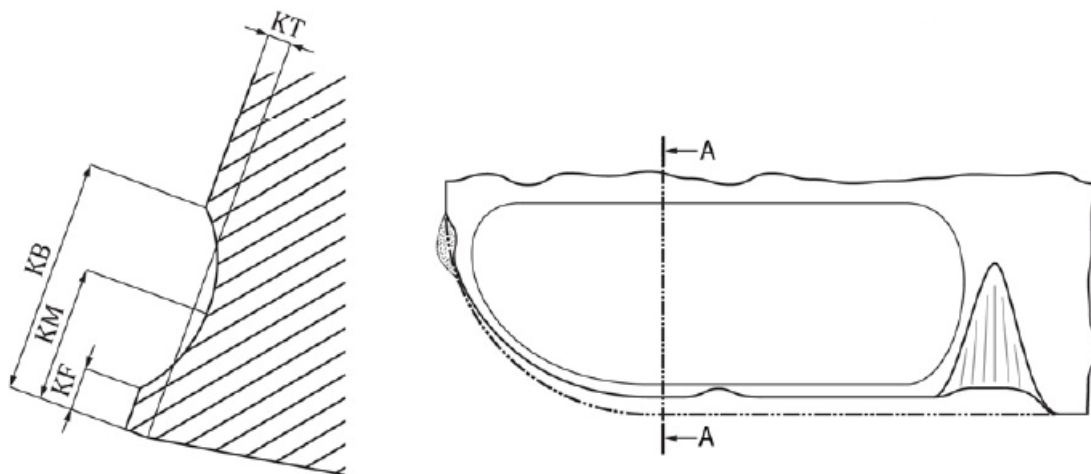


Figure 2-5: Crater wear and measurement ISO 3685:1993

According to PRAMANIK & LITTLEFAIR (2015) when machining Ti-6Al-4V with uncoated cemented tungsten carbide tools, conventional crater wear was seen. However during interrupted machining (milling), tools usually fail due to chipping of the cutting edge because of the high thermal loads and excessive crater wear (OOSTHUIZEN 2010).

2.4.2 Flank Wear

Flank wear on the flank face of the tool is caused by friction between the tool and the machined workpiece surface. Tool pieces adhere to the workpiece surface and are periodically sheared off, which then causes loss of the tool material; this effect increases at higher temperatures. Abrasion is also a dominant mechanism causing flank wear, as grains of work material or tool particles scratch the flank of the tool. (ALTINTAS 2011)

When milling titanium alloys, localized flank wear is the dominant wear mechanism determining tool life of uncoated and coated tools (NOUARI & GINTING 2006). According to JAWAID ET AL. (2000) when face milling Ti-6Al-4V with coated carbide tools, adhesion and diffusion wear mechanisms are responsible for flank wear of the tool.

The measured length on a typical flank wear pattern is the average width of the flank wear land (VB) as it can be seen in Figure 2-6.

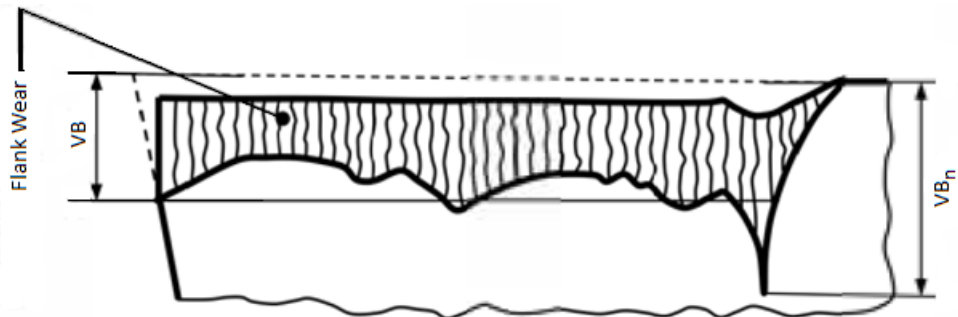


Figure 2-6: Flank wear, notch wear and measurement based on
ISO 3685:1993

2.4.3 Chipping

Chipping is the loss of small particles from the cutting edge of the tool. When milling a workpiece, chipping of the tool is caused by periodical mechanical and thermal shocks. Some cutters with small clearance angles may completely fail after the first chipping, but other cutters with large clearance angles may sustain repeated damage and still continue to cut nicely. (PEKELHARING 1984)

When using coated cutters, chipping may damage the protective coating which would reduce the wear resistance significantly (DOLINŠEK & KOPAČ 2006). According to JAWAID ET AL. (2000) thermal cracks were observed and they were thought to be responsible for severe chipping and flaking of the coated carbide tools when face milling Ti-6Al-4V.

2.4.4 Fracture

According to ALTINTAS (2011) tool fracture is “the loss of a major portion of the tool wedge, which terminates the total cutting ability of the tool” and unlike chipping, fracture of the tool leads to total breakage. Fracture failure may result from high cutting forces, vibration, hard inclusions in the work material, improper exit conditions (foot formation) or thermal shock when milling titanium alloys (STEPHENSON & AGAPIOU 2016, JAWAID ET AL. 2000). According to GU ET AL. (1999) coated tools are more fracture resistant than the uncoated tools.

2.4.5 Notch Wear

According to STEPHENSON & AGAPIOU (2016), notching is caused by abrasive and chemical wear. The measured length on a typical notch wear pattern is the average width of the notch wear (VB_n) as seen in Figure 2-6.

Researches show that when milling Ti-6Al-4V with cryogenic coolants, notch wear dominates tool wear (SADIK ET AL. 2016). According to DEARNLEY & GREARSON (2013) when machining Ti-6Al-4V with ceramic tool materials, notch wear controls tool life but notch wear is infrequently observed when using cemented carbide tools.

When machining Ti-6Al-4V with cubic boron nitride or polycrystalline diamond tools, notch wear is always observed at the limit of the cutting zone. Notch wear could be explained by the accelerated graphitization of the diamond tools, caused by high temperatures combined with low pressure. (CORDUAN ET AL. 2003)

2.4.6 Coating Delamination

Delamination of coating when machining Ti-6Al-4V has been reported by several researchers (NOUARI & GINTING 2006, DEARNLEY & GREARSON 2013, CORDUAN ET AL. 2003). When machining titanium alloys, coating delamination happens due to diffusion or adhesive wear (EZUGWU & WANG 1997).

According to NOUARI & GINTING (2006) when milling an $\alpha+\beta$ titanium alloy with a multi-layer chemical vapor deposition coated carbide tool, coating delamination is found to be the initial wear mechanism, as it occurs after a few minutes of cutting time.

The cutting parameters should be selected carefully when milling with coated carbide tools or inserts. When the cutting speed, depth of cut or the feed rate is too high the coating is directly torn off, causing rapid tool wear. (CORDUAN ET AL. 2003)

2.4.7 Chatter

According to QUINTANA & CIURANA (2011) , "Chatter is a self-excited vibration that can occur during machining operations and become a common limitation to productivity and part quality.".

When milling titanium alloys, chatter results in very poor surface finish and reduced tool life. However tool life can be improved by about a factor of 2 if variable pitch cutters and adaptive controls are used for chatter suppression. (BUDAK & KOPS 2000)

2.5 Modelling and Prediction of Tool Life

Prediction of tool life is important for scheduling tool changes and producing good surface finishes. Since F. W. Taylor first developed an empirical equation for tool life prediction, several researches have been made for developing better models that are capable of describing tool life when machining different workpiece and tool material combinations. Currently there are various tool life prediction models in literature that would predict tool life depending on cutting speed, feed rate, temperature, pressure, hardness, equivalent chip thickness and many other parameters.

It is possible to make 4 main groups from the most important tool life prediction models that could be found in literature. Models will be grouped either by the model that the developed model was based on or the assumptions that were made to develop the model. (BARROW 1972, MÜLLER 1982, ZANGER 2013) In the following sections various tool life prediction models will be grouped and discussed.

2.5.1 Taylor-Type Equations

The well-known tool life equation of TAYLOR (1907) is a function of cutting speed (v_c), tool life (T), tool-workpiece specific constant (α). Which is determined by the slope of the $\log(T)$ - $\log(v_c)$ plot. The so-called Taylor constant (C_T) is the cutting speed for a one minute tool life as shown in Equation 2-4.

$$v_c \cdot T^\alpha = C_T \quad (2-4)$$

Logarithms taken on both sides of Equation 2-4 transforms the equation into a linear estimation problem as seen in Equation 2-5:

$$\ln v_c + \alpha \cdot \ln T = \ln C_T \quad (2-5)$$

Equation 2-4 determined the relationship between the cutting speed and the tool life and ignored the lighter influences of the other cutting parameters, except by changes in the value of the Taylor constant (C_T). However Taylor also connected tool life with feed rate and depth of cut, but did not develop a tool life equation depending on all three cutting parameters. (BARROW 1972, WOLDMAN & GIBBONS 1951)

WOLDMAN & GIBBONS (1951) assumed that the Taylor constant (C_T) would vary with feed rate per tooth (f_z) and depth of cut (a_p) as shown in Equation 2-6.

$$C_1 = \frac{C_T}{a_p^\beta \cdot f_z^\gamma} \quad (2-6)$$

Exponents β and γ are constants that vary with work material and cutting tool.

If equations 2-4 and 2-6 are combined, the result is known as "Extended Taylor Equation", which is a general purpose tool life equation that shows the relationship between tool life (T), cutting speed (v_c), feed rate per tooth (f_z) and depth of cut (a_p) as shown in Equation 2-7 (WOLDMAN & GIBBONS 1951).

$$v_c \cdot T^\alpha \cdot a_p^\beta \cdot f_z^\gamma = C_1 \quad (2-7)$$

According to OXLEY (2007), when selecting optimum cutting conditions "Extended Taylor Equation" is the most widely used tool life equation. Determining the constants α , β and γ is a well-known but also hard task, due to the number of experiments that need to be conducted in order to calculate the value of the constants (YELLOWLEY & BARROW 1971).

2.5.2 Equations Based on Chip-Equivalent Concept

The term "chip-equivalent" was first used by Ragnar Woxén in 1932 and assumes that the actual area of cut (A) at a certain cutting speed and the length of the engaged cutting edge (L) can be used as a proxy for the quantity of heat generated and the quantity of heat carried away, respectively. "The chip-equivalent" q is defined by Woxén as "the physical reality which, together with the cutting speed v_c , and the material constants, determine the temperature Θ , in the nose of the tool". The chip-equivalent q in 1/mm is a function of the length of the engaged cutting edge in mm and the actual area of cut in mm² as it is shown in Equation 2-8. (WOXÉN 1932)

$$q = \frac{L}{A} \quad (2-8)$$

By using chip-equivalent, WOXÉN (1932) developed following tool life equation:

$$v_c = \left[\left(\frac{T_*}{T} \right)^{\alpha_q} + g_1 \cdot T \right] \cdot G_* \cdot \frac{q + q_0}{1 + g_0 \cdot q}, \quad (2-9)$$

Where v_c is the cutting speed, T is an arbitrary tool life, T_* is a certain tool life (e.g. 60min), q is the chip-equivalent, q_0 is a simple function of T , α_q is a function depending on q , G_* is a constant determined by material and tool which referred to the tool life T_* , g_0 is a constant that is equal or greater than 0 and g_1 is a constant.

The first part of the equation $(T_*/T)^\alpha$ represents a straight line in a double logarithmic v_c - T diagram in accordance with the tool life Equation 2-4 of Taylor. However WOXÉN (1932) mentions that in many experiments slightly bent curves were obtained rather than straight lines and the resulting curves had different slopes at different chip-equivalents, which he overcame by adding the term $g_1 * T$. The last part of the equation represents the general dependence of cutting speed upon the chip equivalent with the correction factor $(1/1 + gq)$. (WOXÉN 1932)

According to researchers, Equation 2-9 is valid for a wide range of cutting conditions but rather too complicated for practical use.(WOXÉN 1932, BARROW 1972)

COLDING (1961) suggested a polynomial relationship as seen in Equation 2-10, where tool life was a function of cutting speed and chip-equivalent. However determining nine constants a, b, c, d, e, f, g, h and k required enormous amount of tool life tests (about 25). In the following equation of Colding $x=\ln q$ (chip-equivalent), $y=\ln v_c$ (cutting speed), $z=\ln T$ (tool life).

$$k + y + a \cdot y^2 + b \cdot x + c \cdot x^2 + d \cdot z + e \cdot x^2 + f \cdot x \cdot y + g \cdot y \cdot z + h \cdot x \cdot z = 0 \quad (2-10)$$

Colding proposed another 2nd degree polynomial Equation 2-12 with 5 constants in 1979, where tool life was a function of cutting speed and equivalent chip thickness h_e in mm which is: (COLDING 1991)

$$h_e = q^{-1} = \frac{A}{L} \quad (2-11)$$

$$k + y + b \cdot x + c \cdot x^2 + d \cdot z + h \cdot x \cdot z = 0 \quad (2-12)$$

Both Equations 2-10 and 2-12 are mathematical curve approximations. However Colding recommends the use of the equation 2-12 because of the fact that it requires much less tool life tests to determine the constants. (COLDING 1991)

YELLOWLEY & BARROW (1971) suggested a new extension (Equation 2-13) to the Taylor's equation using the equivalent chip thickness h_e .

$$v_c \cdot T^\alpha \cdot h_e^\delta = C \quad (2-13)$$

In Equation 2-13 tool life is a function of cutting speed v_c and equivalent chip thickness h_e . The tool and workpiece specific constants α , δ and C that need to be determined experimentally.

When comparing Equations 2-7 and 2-13, equivalent chip thickness reduces the number of model constants by taking a balance depth of cut and feed rate. This reduces the number of tests needed to determine the constants, thereby saving costs of tool and work material as well as reducing machine and operator time. Experiments also show that once the constants are determined Equation 2-13 has lower amount of average errors than Equation 2-7. (JOHANSSON ET AL. 2017)

Although the equations of Colding, Yellowley & Barrow are Taylor-Type equations they are based on chip-equivalent concept.

2.5.3 Equations Depending on Pressure and Hardness

HOLM (1946) was one of the first pioneers to develop an empirical equation for abrasive wear assuming that material is removed per individual atoms. In Equation 2-14 the wear volume W is a function of sliding distance (s), hardness of the softer material (H) and the pressure (p). Assuming that the worn off material spreads on the sliding track and forms a coherent film, of which the atomic layers determines the constant Z . (HOLM 1967)

$$W = Z \cdot \frac{p \cdot s}{H} \quad (2-14)$$

BURWELL & STRANG (1952) showed with electron microscope images that, the worn off material is removed as relatively large aggregates of atoms (as particles), and proposed a theory of changing the constant Z with a constant K , which is the probability of removing a wear particle per unit distance of travel as it is shown in Equation 2-15.

$$W = K \cdot \frac{p \cdot s}{H} \quad (2-15)$$

ARCHARD (1953) made assumptions based on the results of HOLM (1946) and BURWELL & STRANG (1952) showing that during a sliding of one cm, a number of contact occur and that the worn volume per effective sliding distance is proportional to the load.

Equations in this section were not specifically made for tool wear, however they were empirical equations describing the amount of wear between the two materials. TRIGGER & CHAO (1956) presented a model for describing crater wear based on Burwell and Strang's equation so that the effects of cutting speed and feed rate are taken into account by introducing normal force N at the tool surface. In Equation 2-16 index i stands for the contact surface, H describes the hardness of the surface asperities.

$$\frac{W_i}{N \cdot s_i} = \left(\frac{K_T}{H} \right)_i \quad (2-16)$$

According to TRIGGER & CHAO (1956), constant K_T in the previous equation is a function of machining temperatures based on Arrhenius Equation 2-17, which can be used for modelling temperature variation of diffusion coefficients.

$$K_T \cdot A_A \cdot e^{\frac{-E_a}{R \cdot \Theta}}, \quad (2-17)$$

Where E_a is the activation energy, R is the universal gas constant and Θ is the temperature.

Although the tool wear model of TRIGGER & CHAO (1956) is a function of normal force, hardness and temperature, it has been grouped into equations depending on pressure and hardness because of the fact that it was based on Burwell & Strang's equation.

2.5.4 Equations Depending on Temperature

Takeyama & Murata classified tool wear in two main groups and developed a model that will describe the amount of tool wear resulting from these two different wear mechanisms. They assumed that the main mechanisms responsible for tool wear were mechanical wear W_a and physicochemical wear W_r . Where mechanical wear being a function of cutting distance L_c , abrasion resistance of the tool material σ_a and physicochemical wear being a function of temperature at the cutting edge Θ and cutting time t_c as shown in Equation 2-18. (TAKEYAMA & MURATA 1963)

$$W = W_a(L_c, \sigma_a) + W_r(\Theta, t_c) \quad (2-18)$$

Further on TAKEYAMA & MURATA (1963) developed a model for physicochemical wear rate based on the equation of TRIGGER & CHAO (1956) assuming that the physicochemical wear is proportional to $e^{-E_a/K\cdot\Theta}$, where E_a is the activation energy, C_{TM} the experimentally determined constant and Θ the temperature. Considering that the abrasive particles in the work material is uniform and always new abrasive particles abrade the tool, Takeyama & Murata concluded that the mechanical wear rate would be proportional to the cutting distance and independent of temperature as seen in the following Equation 2-19:

$$\frac{dW}{dt_c} = v_c(\Theta, f) \cdot A_{TM} + B_{TM} \cdot e^{\frac{-E_a}{C_{TM}\cdot\Theta}}, \quad (2-19)$$

Where A_{TM} and B_{TM} are constants depending on tool and work material, and f the feed.

USUI ET AL. (1978) derived a characteristic equation of crater wear per sliding distance of carbide tools, where the tool life is a function of normal stress on the contact surface σ_t and chip surface temperature Θ . As seen in Equation 2-20 the model of Usui includes the mechanical effects represented by normal stress on the contact surface σ_t and sliding distance L_s .

$$\frac{dW}{\sigma_t \cdot dL_s} = C_1 \cdot e^{\frac{-C_2}{\Theta}}, \quad (2-20)$$

where C_1, C_2 are tool and workpiece depending constants.

2.5.5 Other Models

DEPIERREUX (1969) used a different approach than the other tool life equations. Unlike the tool life equation of TAYLOR (1907) which had constant exponents, Depiereux's equation used exponents that were a function of cutting speed v_c and feed rate per tooth f_z . This way Depiereux determined a function of the slope k_s of $\log(T) - \log(v_c)$ as seen in Equation 2-21.

$$k_s = k_v \cdot v_c^m \quad (2-21)$$

Analog to the Equation 2-21, Depiereux determined a function of the slope i_s of $\log(T) - \log(f_z)$ as seen in Equation 2-22.

$$i_s = i_f \cdot f_z^n \quad (2-22)$$

Where k_v , m , i_f and n are experimentally determined tool and workpiece specific constants. He then calculated partial derivatives of both equations and determined a tool life equation, which was a function of both cutting speed and feed rate per tooth as seen in Equation 2-23.

$$dT = -T \cdot k_v \cdot v_c^{m-1} \cdot dv_c - T \cdot i_f \cdot f_z^{n-1} \cdot df_z \quad (2-23)$$

With the Equation 2-23 curved tool life equations can be determined unlike Taylor's tool life equation. However when the Equation 2-23 is integrated, the integration constant c also needs to be determined, making the total amount of constants five.

HARTUNG ET AL. (1982) developed a tool wear model that would accurately predict the wear rate of polycrystalline diamond and tungsten carbide tools. The model was based on diffusion flux of the stable reaction layer that was formed between tool and workpiece (chip) and was limited to describe diffusion wear. The wear model doesn't use any machining parameters as seen in Equation 2-24.

$$V_{wear} = -\frac{V_t \cdot D_c}{c_t \cdot t} \cdot \left(\frac{c_b}{V_b} - \frac{c_o}{V_o} \right) \quad (2-24)$$

Due to the amount of variables, the variables will be presented and explained in the List of Figures section.

3 Modelling of Tool Wear in Ultrasonic Vibration Assisted Milling

The main goal of this chapter is to develop a tool life model that would be able to describe the effects of longitudinal and torsional ultrasonic vibrations. This chapter will be divided into two main sections.

In the first main section an existing tool life model will be chosen for further development. There will be two main criteria when choosing a tool life model. Finding an equation that can describe wear mechanisms when milling titanium alloy Ti-6Al-4V and an equation that is adequate for extending.

In the second main section, the chosen tool life equation will be extended with maximum equivalent chip thickness in order to describe the effects of conventional milling and ultrasonic vibration assisted milling in a better way.

Then a critical vibration speed will be defined to divide ultrasonic vibration assisted milling into two scenarios. The first case will be modelling the tool life with a periodic tool and workpiece separation due ultrasonic vibration assistance.

The second case will be modeling the tool life without periodic tool and workpiece separation.

3.1 Choosing the Tool Life Model

Various tool life models found in literature were shown in the previous chapter. However, it wasn't easy to find the one, that could describe tool wear when milling a titanium alloy and could be extended to describe the effects of ultrasonic vibration assistance.

Equations depending on tool surface temperature are the latest models that have been developed, but in order to use those models one should first develop a model that would accurately predict the tool surface temperatures.

There are currently no models predicting the tool surface temperatures during ultrasonic vibration assisted milling. Unlike turning, conventional milling is an intermittent cutting process and if right cutting parameters are chosen during ultrasonic vibration assisted milling, tool and work material periodically lose contact during a single cut. This situation makes it harder to develop an accurate model to calculate the tool surface temperatures.

Equations depending on pressure and hardness are empirical equations describing the abrasive and adhesive wear and can be used to describe some of the wear mechanisms during ultrasonic vibration assisted milling. However, according to HARTUNG ET AL. (1982) when

machining titanium alloys, most of the tool materials either dissolve or chemically react with titanium. JAWAID ET AL. (2000) mentions that when milling titanium alloys, common tool failure modes are chipping and flaking resulting from high thermo-mechanical cyclic stress. Therefore, just by using Equation 2-14 or 2-15 main tool wear mechanisms during ultrasonic vibration assisted milling of Ti-6Al-4V cannot be properly explained.

Taylor-type equations can be extended for developing a new tool life model that can explain effects of ultrasonic vibrations during milling. However the well-known Equation 2-4 only uses cutting speed as a machining parameter, therefore the effects of depth of cut and feed rate cannot be seen directly.

The extended Taylor Equation 2-7 uses all three machining parameters as mentioned before. However, extending the equation to show the effects of ultrasonic vibrations would add at least one more constant, that needs to be determined experimentally. Considering that the extended Taylor equation already has four constants, adding any more constants would increase the amount of tests needed to determine the constants significantly.

Colding's Equation 2-12 produces better results than Equations 2-4, 2-7 and 2-13. However Colding's equations are both based on mathematical curve adjustments and Equation 2-12 needs 5 constants to be determined experimentally without considering effects of ultrasonic vibrations. Therefore the use of the equation is quite costly. (JOHANSSON ET AL. 2017)

Yellowley & Barrow's Equation 2-13 is so to say a hybrid equation, it is based on the chip-equivalent concept and is a Taylor-type equation. Although the model only needs three constants to be determined experimentally, it outperforms both Taylor and extended Taylor equations by using the chip equivalent concept (JOHANSSON ET AL. 2017).

Our model of choice to extend for ultrasonic vibration assisted milling is the Equation 2-13 developed by YELLOWLEY & BARROW (1971). Equivalent chip thickness concept is used for modelling both tool wear and temperature relations. By choosing flank or crater wear (or both) as a tool life criteria the model could be used to describe different dominant wear mechanisms.

3.2 Extending the Tool Life Model for Ultrasonic Vibration Assisted Milling

3.2.1 Modelling the Maximum Equivalent Chip Thickness in Milling

WOXÉN (1932) defined the chip equivalent as it was discussed in the previous chapter. Later the chip equivalent was inverted to the equivalent chip thickness and used by YELLOWLEY & BARROW (1971) in tool life equations, as it combined depth of cut and feed rate into a single variable and produced accurate results with less constants that need to be determined experimentally. However, WOXÉN (1932) only determined an approximation for the chip equivalent in turning which is given in Equation 3-1. According to WOXÉN (1932) the chip equivalent q for turning is a function of feed per revolution f_r , depth of cut a_p , major cutting angle K and the tool nose radius of the tool r_e .

$$q = \frac{a_p \cdot f_r}{\frac{a_p - r_e \cdot (1 - \cos(K))}{\sin(K)} + K \cdot r_e + \frac{f_r}{2}} \quad (3-1)$$

Unlike turning, milling is characterized by varying but periodic chip thickness. This results in periodically changing length of the engaged cutting edge and actual area of cut. Because of this the chip equivalent equation done for turning cannot be used in milling. The varying chip thickness needs to be modelled to produce an accurate equivalent chip thickness model for milling.

COLDING (1961), did the only research to model the chip equivalent in milling, which he called "the milling equivalent for face milling m_f ". In order to describe the varying area of cut and the undeformed chip thickness during milling, Colding introduced the terms "characteristic cross-sectional area of cut A_c " and "characteristic depth of cut h_c ", where the characteristic depth of cut is an approximation for undeformed chip thickness. Both terms are derived from the volume continuity equation and they are a function of cutting speed v_c , feed rate f , axial depth of cut a_p and radial depth of cut a_e as seen in Equations 3-2, 3-3 and 3-4.

$$\frac{dW}{dt} = v_c \cdot A_c = v_c \cdot a_p \cdot a_e \quad (3-2)$$

$$A_e = \frac{f}{v_c} \cdot a_p \cdot a_e \quad (3-3)$$

$$h_c = \frac{A_c}{a_p} = \frac{f}{v_c} \cdot a_e \quad (3-4)$$

By using the characteristic depth of cut h_c , axial depth of cut a_p and the helix angle of the carbide cutter β , the length of the engaged cutting edge L can be calculated for the carbide tool that has been used in experiments as seen in Equation 3-5.

$$L = h_c + \frac{a_p}{\cos(\beta)} \quad (3-5)$$

By using the length of the engaged cutting edge L , the milling equivalent for face milling m_f can be found. However, COLDING (1961) did not use the characteristic cross-sectional area of cut A_c when calculating face milling equivalent. The area of cut A is calculated by multiplying the characteristic depth of cut h_c with axial depth of cut a_p as seen in Equation 3-6.

$$m_f = \frac{L_c}{A} = \frac{h_c + a_p / \cos(\beta)}{h_c \cdot a_p / \cos(\beta)} = \frac{f/v_c \cdot a_e + a_p / \cos(\beta)}{f/v_c \cdot a_e \cdot a_p / \cos(\beta)} \quad [mm] \quad (3-6)$$

The Equations 3-5 and 3-6 were developed analog to Colding's equations, because of the different carbide cutter geometries used during experimental validation.

In this thesis we will be working with torsional and longitudinal ultrasonic vibration producing milling machine. Our main focus in this thesis will be modelling torsional and longitudinal vibrations effects on tool life. However considering the direction and the amplitude of vibrations, there will be almost no considerable change in the undeformed chip thickness and using Colding's milling equivalent in a tool life model should give satisfying results.

Colding uses characteristic depth of cut to find an average value for the varying chip thickness. However wear maps for milling Ti-6Al-4V developed by OOSTHUIZEN (2010) show that the maximum undeformed chip thickness is associated with catastrophic tool failure. Therefore by modelling the equivalent chip thickness where it reaches the maximum undeformed chip thickness may lead to a more accurate tool life equation.

To find out the tool position (angle), where the maximum undeformed chip thickness in a face milling operation is reached, paths made by two following flute corners (cutting patterns of the milling cutter) will be modelled in a simple way. By having a third function, which will describe position of the tools end cutting edge as a function of rotation angle one would be able to find the value and the location of the maximum undeformed chip thickness.

Variables to be used for modelling flute corners and end cutting edge will be; the feed rate per tooth f_z , number of flutes z and tool radius r . If the feed rate per tooth is considered zero, the corners of the tool flutes will create a half circle on the work plane, produced by the rotational movement of the tool. However if the feed rate per tooth is greater than zero the tool will turn and at the same time move in the feed direction, causing a deformed half circle. The deformed half circle is the path made by a single flute of the milling cutter as seen in Equation 3-7.

$$c_1(x) = \sqrt{r^2 - x^2} + f_z \cdot \frac{z}{2} \cdot \frac{x + r}{2 \cdot r} \quad (3-7)$$

The first part of the equation creates a half circle, second part of the equation is the distance between the two ends of the circle in feed direction and the last part of the equation models the linear movement of the tool in feed direction (y-axis).

Analog to the Equation 3-7, path of the following flute can be modelled by adding the feed rate per tooth f_z , as seen in Equation 3-8.

$$c_2(x) = \sqrt{r^2 - x^2} + f_z \cdot \frac{z}{2} \cdot \frac{x + r}{2 \cdot r} + f_z \quad (3-8)$$

The position of the end cutting edge can be calculated by knowing the feed rate per tooth f_z , number of flutes z and current angle of the end cutting edge α in radian. End cutting edge can be modelled as a straight line, that rotates due to the spinning tool and moves in the feed direction. In Equation 3-9 the position of the second flutes end cutting edge is modelled.

$$e_2(x, \alpha) = |\tan(\alpha) \cdot x| + f_z \cdot \frac{z}{2} \cdot \frac{\alpha}{\pi} + f_z \quad (3-9)$$

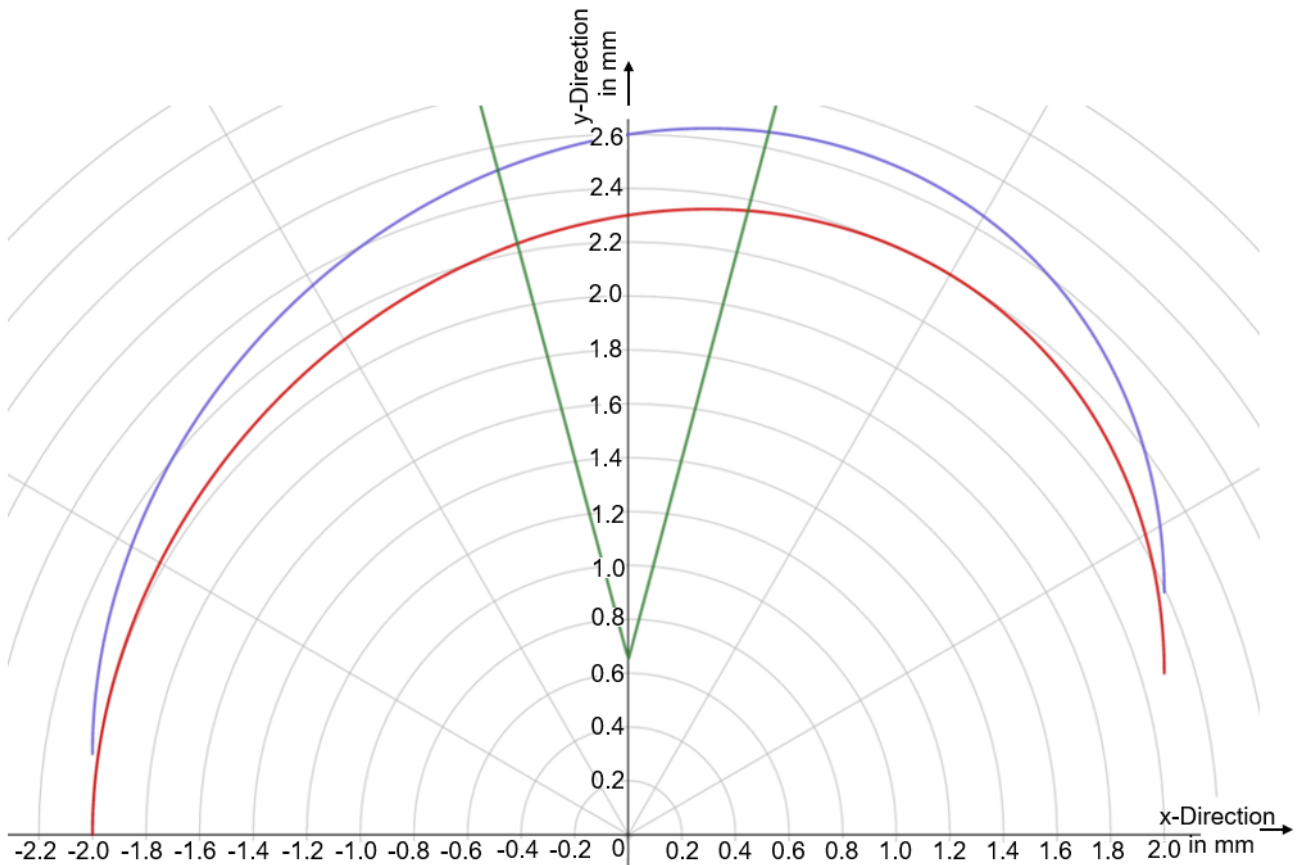


Figure 3-1: Varying undeformed chip thickness for a slotting operation

First part of the Equation 3-8 creates a straight line with a slope of α , second part of the equation models the linear movement of the milling cutter in feed direction.

In Figure 3-1 the Equations 3-7, 3-8 and 3-9 are graphed for a four flute tool (z) with a 2mm radius (r), 0.3mm feed per tooth (f_z) and current tool angle at $7/12\pi$ (105°). The red curve indicates the cut done by the first flute (Equation 3-7), blue curve indicates the cut done by the second flute (Equation 3-8) and the green lines demonstrate the current location of the end cutting edge (Equation 3-9). Y-axis is the feed direction.

The equivalent chip thickness in any given angle can be calculated by finding the intersection points of both tool paths with the end cutting edge position. Which is done by solving Equations 3-10 and 3-11 for both intersection points x_{i1} and x_{i2} respectively.

$$\sqrt{r^2 - x_{i1}^2} + f_z \cdot \frac{z}{2} \cdot \frac{x_{i1} + r}{2 \cdot r} = |\tan(\alpha) \cdot x_{i1}| + f_z \cdot \frac{z}{2} \cdot \frac{\alpha}{\pi} + f_z \quad (3-10)$$

$$\sqrt{r^2 - x_{i2}^2} + f_z \cdot \frac{z}{2} \cdot \frac{x_{i2} + r}{2 \cdot r} = |\tan(\alpha) \cdot x_{i2}| + f_z \cdot \frac{z}{2} \cdot \frac{\alpha}{\pi} \quad (3-11)$$

However, as seen in Figure 3-1 both of the equations provide two possible values for an intersection point. For a face milling operation or for a side milling operation with a sweep angle greater than $\pi/2$, the result with the positive sign should be calculated numerically and used for determining the undeformed chip thickness. For a side milling operation with a sweep angle less than $\pi/2$, the sweep angle can be set as the current tool location α and by using the other milling parameters, equations can be solved analytically for x_{i1} and x_{i2} . The Undeformed chip thickness h_{ud} would be the distance between the intersection points and can be calculated by Equation 3-12 and for . For a side milling operation with a sweep angle less than $\pi/2$.

$$h_{ud} = \sqrt{(x_{i2} - x_{i1})^2 + (e_2(x_{i2}) - e_2(x_{i1}))^2} \quad (3-12)$$

For face milling operations, Equations 3-10 and 3-11 cannot be solved analytically for x_{i1} and x_{i2} respectively. By using an iterative approach approximate values for x_{i1} and x_{i2} can be derived. If one can divide the sweep angle into say 10 intervals and calculate the undeformed chip thickness for the beginning and ending angle of these intervals, the maximum undeformed chip thickness will be in the interval that begins and ends with the highest undeformed chip thickness. If the iteration is done once again for the interval with the maximum chip thickness, the highest undeformed chip thickness that is found can be used as the maximum undeformed chip thickness.

By using the maximum undeformed chip thickness $h_{ud,Max}$ and axial depth of cut a_p one can calculate the maximum length of the engaged cutting edge L_{Max} and the maximum area of cut A_{Max} . In order to have a better approximated equations, the helix angle β and the tool nose radius r_n should be also considered as seen in Equations 3-13 and 3-14.

$$L_{Max} = (h_{ud,Max} - r_n) + \frac{a_p - r_n}{\cos(\beta)} + \frac{\pi \cdot r_n}{2} \quad [mm] \quad (3-13)$$

$$A_{Max} = \frac{(h_{ud,Max} \cdot a_p) + \frac{\pi \cdot r_n^2}{4} - r_n^2}{\cos(\beta)} \quad [mm^2] \quad (3-14)$$

It should be noted that the Equations 3-13 and 3-14 are approximations, due to the fact that the undeformed chip thickness will change slightly because of the helix angle. A minor error occurs during calculation of the maximum engaged cutting edge length, because of the tool nose radius and the helix angle. According to YELLOWLEY & BARROW (1971) the use of equivalent chip thickness and the chip equivalent concepts are based on approximations therefore, a more accurate model of the engaged cutting edge length and area of cut shouldn't be necessary. By using the Equations 3-13 and 3-14 the maximum equivalent chip thickness $h_{eq,Max}$ can be calculated as seen in Equation 3-15.

$$h_{eq,Max} = \frac{A_{Max}}{L_{Max}} = \frac{\frac{(h_{ud,Max} \cdot a_p) + \frac{\pi \cdot r_n^2}{4} - r_n^2}{\cos(\beta)}}{(h_{ud,Max} - r_n) + \frac{a_p - r_n}{\cos(\beta)} + \frac{\pi \cdot r_n}{2}} \quad [mm] \quad (3-15)$$

By using the maximum equivalent chip thickness, tool life Equation 2-13 of YELLOWLEY & BARROW (1971) can be extended to model the tool life in face milling operations as seen in Equation 3-16. The tool and workpiece specific constants α , δ and C need to be determined experimentally.

$$v_c \cdot T^\alpha \cdot h_{eq,Max}^\delta = C \quad (3-16)$$

3.2.2 Modelling the Phase With Periodic Tool and Workpiece Separation

Less tool wear during ultrasonic vibration assisted machining was reported by researchers, when ultrasonic vibration velocity in the cutting direction exceeded the cutting speed. Higher vibration speed caused periodic separation of tool and workpiece, which then resulted in lower cutting forces and tool wear. As the cutting speed increased or the amplitude and the frequency of the ultrasonic vibration was lowered, these effects began to diminish because of the increased tool workpiece contact ratio. (NATH & RAHMAN 2008)

Modelling the contact ratio is crucial for describing the tool wear, as it shows a relation with tool life and limits the use of ultrasonic vibration assistance in machining. In this thesis we will be working and modelling the effects of ultrasonic vibrations in longitudinal and torsional directions which can be seen in Figure 3-2.

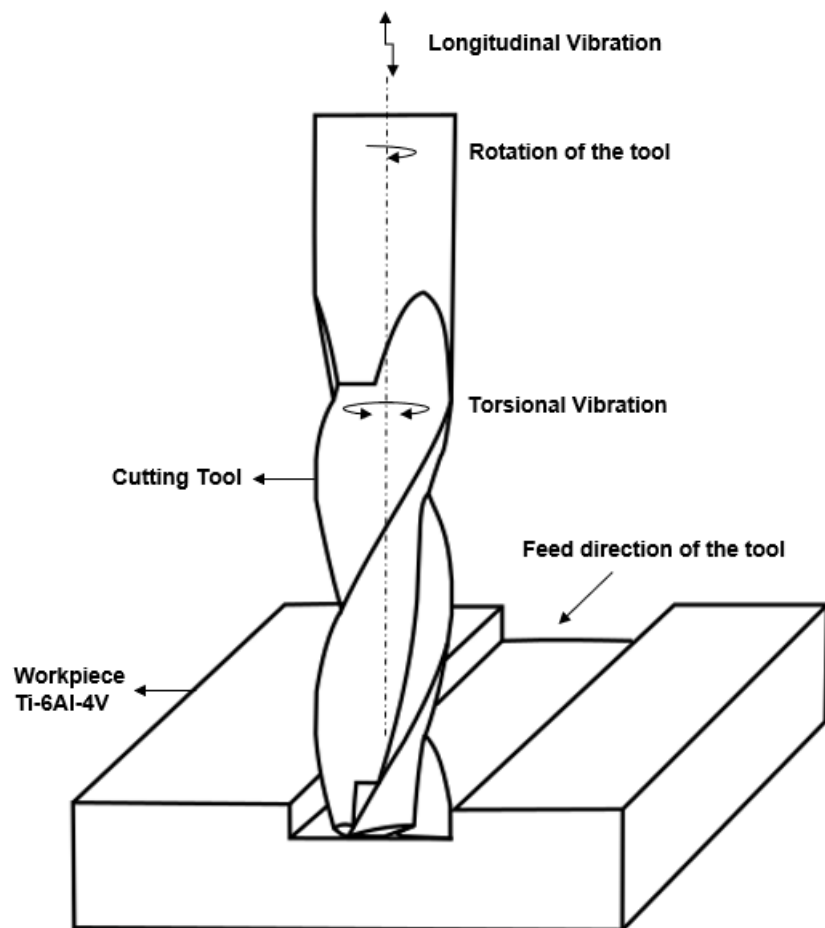


Figure 3-2: Torsional and longitudinal ultrasonic vibration assisted face milling

Following equations leading to the contact ratio in longitudinal and torsional vibration assisted milling will be explained according to BIGELMAIER (2017).

Cutting speed as seen in Equation 2-1 is a function of spindle speed and tool diameter and has a constant value during the milling process. However, the velocity resulting from the ultrasonic vibrations oscillate between their maximum values. To lose contact between tool and workpiece, the sum of both vibration speeds in the cutting direction should be greater than the cutting speed.

The velocity vector resulting from the torsional vibration follows the path of the cutting speed, resulting in a periodic rotation of the tool in positive and negative direction. The milling cutter doesn't rotate because of the longitudinal vibration because the oscillation is normal to the direction of the cutting speed. However, it does periodically move up and down, causing tool and workpiece to lose contact because of the helix angle of the tool.

Position vector resulting from a periodic, harmonic oscillation is a function of time t , oscillation amplitude A_{os} , oscillation frequency f_{os} can be calculated by Equation 3-17.

$$x(t) = A_{os} \cdot \sin(2 \cdot \pi \cdot f_{os} \cdot t) \quad (3-17)$$

The derivation of Equation 3-17 with respect to time t gives the speed vector (v_{os}) as seen in Equation 3-18.

$$v_{os}(t) = 2 \cdot \pi \cdot f_{os} \cdot A_{os} \cdot \cos(2 \cdot \pi \cdot f_{os} \cdot t) \quad (3-18)$$

So the maximum oscillation speed $v_{os,max}$ resulting from a vibration is a function of oscillation frequency and oscillation amplitude as seen in Equation 3-19.

$$v_{os,max} = 2 \cdot \pi \cdot f_{os} \cdot A_{os} \quad (3-19)$$

Equation 3-7 can be used for calculating maximum speed resulting from torsional vibration. If the maximum torsional vibration speed is greater than cutting speed, tool and workpiece periodically lose contact.

On the other hand, just by using the Equation 3-19 we cannot model the vibration speed in cutting direction resulting from longitudinal vibrations as the oscillations normal to the cutting speed direction don't cause the tool to rotate. So the relationship between the helix angle and the longitudinal vibrations need to be modelled to find the critical longitudinal cutting speed that causes contact loss.

The trigonometric relation between the longitudinal vibration and the helix angle β is given in Equation 3-8, where $A_{l,z}$ is the movement of a fixed point on the tool in axial direction, produced by longitudinal vibrations and $\Delta x_{os,l}$ is the distance between the recently cut workpiece surface and the surface of the helical milling cutter, caused by the relative movement of the tool against workpiece in negative z-direction as visualized in Figures 3-3 and 3-4.

Fehler! Verwenden Sie die Registerkarte 'Start', um Heading 1 dem Text zuzuweisen, der hier angezeigt werden soll.

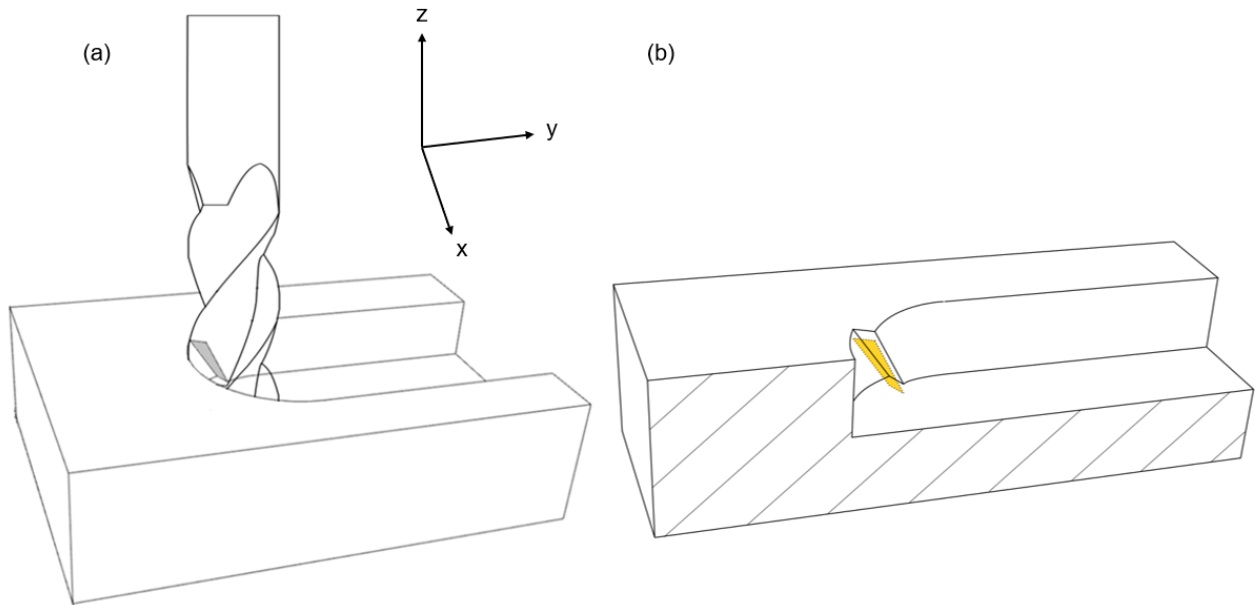


Figure 3-3: Slotting with carbide milling cutter (left), Visualization of tool workpiece separation during longitudinal vibration assisted milling (right)

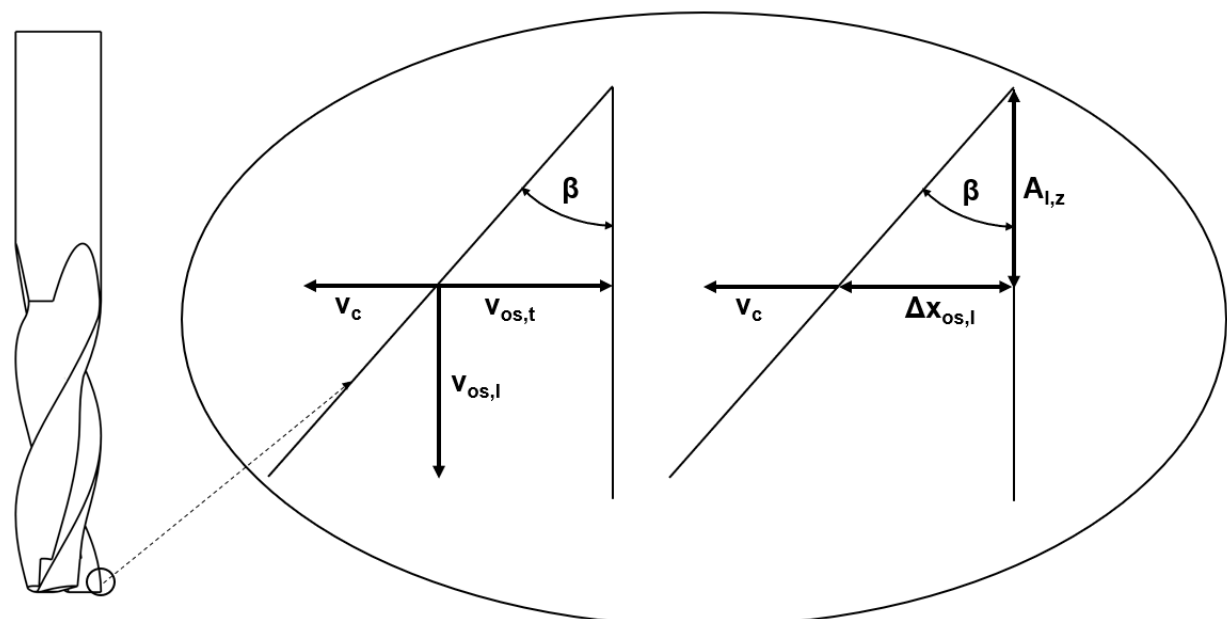


Figure 3-4: Influence of helix angle to contact time according to BIGELMAIER (2017)

$$\tan(\beta) = \frac{\Delta x_{os,l}}{A_{l,z}} \quad (3-20)$$

In Figure 3-3 left side the grey marked section is the area being cut during a slotting operation. In Figure 3-3 right side contact loss during longitudinal vibration assisted milling is visualized, where the yellow marked section is the tools rake face, that had a contact with the workpiece and is separated from the recently cut area by a distance of $\Delta x_{os,l}$ uniformly, which again can be calculated by the Equation 3-20.

The movement of a fixed point on the tool $A_{l,z}$ is equal to the amplitude of the longitudinal oscillation and by knowing the relation between the distance $\Delta x_{os,l}$ and helix angle β (Equation 3-20), the distance between the tools rake face and the area that has been recently cut $\Delta x_{os,l}$ can be written as a function of time t as seen in Equation 3-21.

$$\Delta x_{os,l}(t) = A_l \cdot \tan(\beta) \cdot \sin(2 \cdot \pi \cdot f_{os} \cdot t) \quad (3-21)$$

The derivation of Equation 3-21 with respect to time t provides so to say the speed vector in cutting direction $v_{os,l}$ caused by longitudinal vibrations as seen in Equation 3-22.

$$v_{os,l}(t) = 2 \cdot \pi \cdot f_{os} \cdot A_l \cdot \tan(\beta) \cdot \cos(2 \cdot \pi \cdot f_{os} \cdot t) \quad (3-22)$$

So the maximum oscillation speed in cutting direction $v_{os,l,max}$ resulting from longitudinal vibrations is a function of oscillation frequency f_{os} , longitudinal oscillation amplitude A_l and helix angle of the carbide tool β as seen in Equation 3-23.

$$v_{os,l,max} = 2 \cdot \pi \cdot f_{os} \cdot A_l \cdot \tan(\beta) \quad (3-23)$$

In Equation 3-24, the critical oscillation speed $v_{os,crit}$ resulting from longitudinal and torsional vibrations is determined by combining Equations 3-19 and 3-23. The critical oscillation speed needs to be greater than the cutting speed v_c to break the tool-workpiece contact. Remember that the Equation 3-24 is only valid when there is no phase difference between both vibrations.

$$v_{os,crit} = 2 \cdot \pi \cdot f_{os} \cdot (A_t + A_l \cdot \tan(\beta)) \quad (3-24)$$

If the critical oscillation speed is greater than the cutting speed, there will be periodic loss of contact between the tool and workpiece. A possible way to model this periodic loss of contact is to determine a contact ratio T_c , and to do this three terms are defined, which will be the period duration t_p being a function of oscillation frequency f_{os} , the contact duration t_c , and the duration of tool workpiece separation t_{nc} . The relation between these three terms and contact ratio can be seen in Equations 3-24, 3-26 and 3-27.

$$T_c = t_c / t_p \quad (3-25)$$

$$t_p = 1 / f_{os} \quad (3-26)$$

$$t_p = t_c + t_{nc} \quad (3-27)$$

By determining the moment when the tool enters t_{e1} and exits t_{e2} the workpiece, the contact duration t_c can be calculated as seen in Equation 3-28.

$$t_c = t_p + t_{e2} - t_{e1} \quad (3-28)$$

The tool and workpiece separate when the oscillation speed resulting from longitudinal and torsional vibrations in the negative cutting direction is equal to the cutting speed. To find tool workpiece separation time, the oscillation speed resulting from torsional and longitudinal oscillations in cutting direction v_{UV} is determined as a function of time t , which can be done by adding Equations 3-18 and 3-19 as seen in Equation 3-29. Assuming that there is no phase difference between both vibrations.

$$v_{UV}(t) = 2 \cdot \pi \cdot f_{os} \cdot (A_l \cdot \tan(\beta) + A_t) \cdot \cos(2 \cdot \pi \cdot f_{os} \cdot t) \quad (3-29)$$

When the oscillation speed resulting from torsional and longitudinal oscillations in negative cutting direction is equal to the constant (and positive) cutting speed v_c , relative speed between tool and workpiece in the cutting direction will be equal to zero, resulting the separation of tool and workpiece. The moment at which the tool exits (t_{e2}) from the workpiece and can be found by solving Equation 3-30.

$$(A_l \cdot \tan(\beta) + A_t) \cdot 2 \cdot \pi \cdot f_{os} \cdot \cos(2 \cdot \pi \cdot f_{os} \cdot t_{e2}) = -v_c \quad (3-30)$$

However, the Equation 3-30 has two possible results for t_{e2} when, $0 < t_{e2} < 1/f_{os}$ one being the separation time and the other being time when the tool and workpiece have maximum distance. The result with the smaller value will be the time of separation between tool workpiece t_{e2} .

After the separation of tool and workpiece, the cutting edge of tool will first move to the negative cutting direction, as the absolute value of the resulting oscillation speed is greater than the cutting speed. Maximum distance between tool and workpiece will be reached, when the sum of the resulting longitudinal and torsional oscillation speeds in negative cutting direction is equal to the cutting speed. After the maximum tool workpiece distance is reached, the cutting edge will be moving towards last cut workpiece surface. The tool and workpiece are reunited when there is no distance between the rake face of the tool and the last cut workpiece surface.

The moment of tool workpiece contact (tool entry time) t_{e1} , can be calculated by the Equation 3-31. The Equation 3-31 is based on the assumption that, the distance travelled by the resulting longitudinal and torsional oscillations in negative cutting direction over a certain time ($t_{e1}-t_{e2}$), is equal to the distance travelled by the cutting speed over a certain time ($t_{e1}-t_{e2}$).

$$\Delta x_{os,t} + \Delta x_{os,l} = v_c \cdot (t_{e1} - t_{e2}) \quad (3-31)$$

The distances $\Delta x_{os,t}$ and $\Delta x_{os,l}$ can be calculated by Equations 3-17 and 3-21 respectively, resulting Equation 3-31.

$$A_t \cdot (\sin(2 \cdot \pi \cdot f_{os} \cdot t_{e1}) - \sin(2 \cdot \pi \cdot f_{os} \cdot t_{e2})) + A_l \cdot \tan(\beta) \cdot (\sin(2 \cdot \pi \cdot f_{os} \cdot t_{e1}) - \sin(2 \cdot \pi \cdot f_{os} \cdot t_{e2})) = v_c \cdot (t_{e1} - t_{e2}) \quad (3-32)$$

Although the moment of tool exit t_{e2} can be calculated analytically from the Equation 3-29 the tool entry time t_{e1} can only be numerically approximated from Equation 3-31 and by using Equations 3-25, 3-26 and 3-28 the contact ratio T_c , can be found.

Periodic loss of contact helps the tool to release stresses, reduces the forces and decreases wear by providing interfacial lubrication, decreases tool workpiece contact time leaving less time for the wear mechanisms therefore, increasing tool life. Separation of tool and workpiece allows the tool to cool down which increases the tool life especially for hard to machine materials like Ti-6Al-4V. (KUMAR ET AL. 2014, TSAI ET AL. 2016)

Therefore by decreasing the tool-workpiece ratio T_c one should be able to reach longer tool life. This results an inverse proportionality between the tool life and tool to workpiece contact ratio which can be used in tool life equations to describe the effects of ultrasonic vibrations on tool life. By using contact ratio we can extend the Equation 3-16 (that was improved for describing tool life in conventional milling in the previous section) of YELLOWLEY & BARROW (1971), to model tool life in ultrasonic vibration assisted milling with periodic tool-workpiece separation as seen in Equation 3-33.

$$v_c \cdot T^\alpha \cdot h_{eq,Max}^\delta \cdot T_c^\gamma = C \quad (3-33)$$

Where exponents α , δ , γ and C are tool and workpiece specific constants that are needed to be determined experimentally.

3.2.3 Modelling the Phase Without Tool and Workpiece Separation

In torsional and longitudinal vibration assisted milling, if the required frequency and amplitude combination is not reached, tool and workpiece wouldn't separate due to the combined vibration speed in cutting direction being always lower than the cutting speed itself. The critical speed combining vibration amplitudes and oscillation frequency is given Equation 3-11 in the previous section. However, even if the critical combined vibration speed is not reached, tool and workpiece separation at end cutting edge will occur because of the longitudinal vibrations. If the mentioned critical speed is not higher than the cutting speed a conventional milling alike tool life will occur.

Tool life can be even shorter if no tool and workpiece separation occurs, SUÁREZ ET AL. (2016) did longitudinal vibration assisted face milling experiments with nickel alloy 718 and observed 10% greater flank wear than conventional milling. However, LI ET AL. (2012) did longitudinal vibration assisted end milling experiments with high carbon, high chromium alloy steel STD11 and showed that the tool used in vibration assisted experiments developed less tool wear than the one used in conventional milling experiments.

One can still benefit from other aspects of ultrasonic vibration assisted milling, HEISEL ET AL. (2014) mentioned, when slotting 42CrMo4 without any tool and workpiece separation the forces were reduced by 30% and the Ra roughness was respectively reduced by 10% and this can be achieved with respect to the conventional milled workpieces. However, SUÁREZ ET AL. (2016) observed approximately a 25% increase of the Ra roughness but almost 15% higher fatigue life of the workpiece with respect to the conventional milling.

Assuming that, by using vibration assistance when milling titanium alloys, there will be extra energy transferred to the tool tip due to the ultrasonic vibrations. The low thermal conductivity of Ti-6Al-4V and the extra energy transferred to the tool can cause higher temperatures without any tool and workpiece separation, which then can cause higher diffusion and chemical reactions increasing the crater wear rate of the tool.

Temperatures higher than conventional machining were reported by several researchers when using ultrasonic vibration assisted machining even with a critical vibration speed in cutting direction being higher than the cutting speed (or feed rate, depending on the direction of the vibration) causing interrupted cutting (NATEGH ET AL. 2009, PUJANA ET AL. 2009).

In Figure 3-5 theoretical tool wear locations during ultrasonic vibration assisted milling without any tool and workpiece separation is explained on a carbide cutter illustration. In Figure 3-5 the red marked areas indicate more wear and yellow marked areas indicate less tool wear. Theoretical reasons for more or less tool wear will be explained in the following paragraphs.

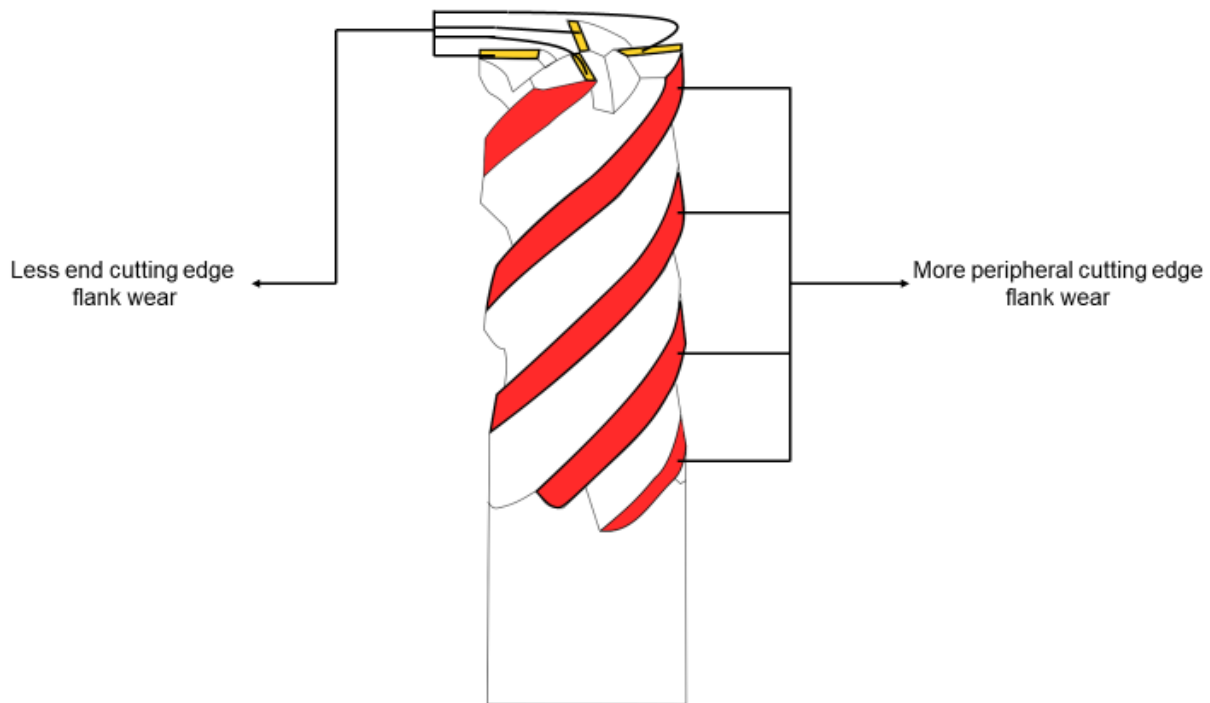


Figure 3-5: Theoretical amounts of tool wear during ultrasonic vibration assisted milling

Considering that there were almost no information found in literature, describing the exact mechanisms that caused the tool to wear faster or slower than conventional milling when milling with ultrasonic vibration assistance under the critical vibration speed. There are two different assumptions that could be made to describe the tool life.

The first assumption will be for explaining the shorter tool life due to the ultrasonic vibrations. The first reason for shorter tool life, would be higher temperatures in tool chip interface caused by ultrasonic vibrations. Higher temperatures can cause thermal softening, therefore increase plastic deformation of the tool tip or cause the tool to wear faster due to crater wear by speeding up the diffusion process. Crater wear is one the most common tool wear modes in conventional turning of Ti-6Al-4V.

However, the main failure modes during milling Ti-6Al-4V are plastic deformation of the tool cutting edge and the flank wear. More peripheral cutting edge fractures and flank wear during vibration assistance can be explained by the tool hitting the machined surface and increased rubbing caused by ultrasonic vibrations respectively. This way we can explain the increased flank wear that was mentioned by SUÁREZ ET AL. (2016) when longitudinal vibration assisted face milling nickel alloy 718.

The mentioned tool wear mechanisms should then theoretically rise by increasing the frequency and amplitude of the ultrasonic vibrations. However, with an increasing cutting speed, the speed caused by the ultrasonic vibrations should play a relatively minor role on the tool wear. Meaning the ratio between the cutting speed and the combined velocities of the ultrasonic vibrations should be a better indicator for tool life. Therefore, the tool life should be thereby inversely proportional to the ratio between vibration speed and the combined velocities of the ultrasonic vibrations.

Combined velocities of longitudinal and torsional vibrations $v_{UV,co}$ can be found by adding resulting speeds of both oscillations as seen in Equation 3-34.

$$v_{UV,co} = 2 \cdot \pi \cdot f_{os} \cdot (A_t + A_l) \quad (3-34)$$

The destructive effects of ultrasonic vibrations can be explained by multiplying tool life equation of YELLOWLEY & BARROW (1971) extended for milling (Equation 3-16) with the ratio between tool cutting speed and combined vibration speeds. However, the effects caused by cutting speed v_c and combined vibration speed $v_{UV,co}$ ratio may vary with different tool and workpiece combinations, so a constant exponent γ is added to the equation that needs to be found experimentally as seen in Equation 3-35.

$$v_c \cdot T^\alpha \cdot h_{eq,Max}^\delta \cdot \left(\frac{v_c}{v_c + v_{UV,co}} \right)^\gamma = C \quad (3-35)$$

Where exponents α , δ , γ and C are tool and workpiece specific constants that are needed to be determined experimentally.

The second assumption will be for explaining longer tool life due to ultrasonic vibrations. Longer tool life can be an effect of lower forces that occur during ultrasonic vibration assisted milling even when tool workpiece separation do not occur. Catastrophic tool failures like fracture or tool tip breakage usually occur because of high machining forces. LI ET AL. (2012) did longitudinal vibration assisted milling experiments with high carbon, high chromium alloy steel STD11 and observed less fracture wear than conventional milling.

Less catastrophic tool failures can be achieved by low machining forces. According to HEISEL ET AL. (2014) machining forces decrease with increasing vibration frequency and assuming that the machining forces will also decrease by increasing the vibration frequency, tool life should have a proportional relationship with the combined vibration velocities. However, with an increasing cutting speed, the ultrasonic vibrations should have less influence on the cutting forces. Therefore the ratio between the combined velocities of the ultrasonic vibrations and the cutting speed should be an optimal indicator for tool life.

However, the effects caused by combined vibration speed $v_{UV,co}$ and cutting speed v_c ratio may vary with different tool and workpiece combinations, so a constant exponent γ is added to the equation that needs to be found experimentally as seen in Equation 3-36.

$$v_c \cdot T^\alpha \cdot h_{eq,Max}^\delta \cdot \left(\frac{v_c + v_{UV,co}}{v_c} \right)^\gamma = C \quad (3-36)$$

Where exponents α , δ , γ and C are tool and workpiece specific constants that are needed to be determined experimentally.

The Equations 3-35 and 3-36 are quite similar, the difference between them can be also explained by the material specific constant γ having a negative value. Because of the contradictory information's that were found in literature about tool wear in ultrasonic vibration assisted milling without tool and workpiece separation, one cannot tell which one would describe tool life better.

However, if the material specific constants of both Equations 3-35 and 3-36 are determined with exactly the same data, one of the equations will have a negative value for constant γ and the other one will have positive value and the absolute value of the constant γ , which is determined for 2 different equations will be the same. This situation would make both equations able to describe the tool life when ultrasonic vibration assisted milling without periodic tool-workpiece separation.

4 Experimental Validation

This chapter is for verifying proposed models in chapter 3. For the validation, experiments were conducted in a 5-Axis machine with ultrasonic vibration capabilities. The used equipment and settings are described in the first section. Afterwards, the experimental approach for the tool life tests will be explained and the results of conventional and ultrasonic vibration assisted milling experiments will be compared in the second section.

4.1 Experimental Equipment and Setting

Experiments that were required for determining the tool and workpiece specific constants and for the validation were carried out on a DMG MORI Ultrasonic 40 5-Axis CNC Milling Center. Used milling center is equipped with rotary ultrasonic machining capabilities for conventional and ultrasonic vibration assisted milling. Workspace of the used machine and the experimental setup done for longitudinal (coaxial direction to the main spindle) vibration amplitude and frequency measurements can be seen in the Figure 4-1.

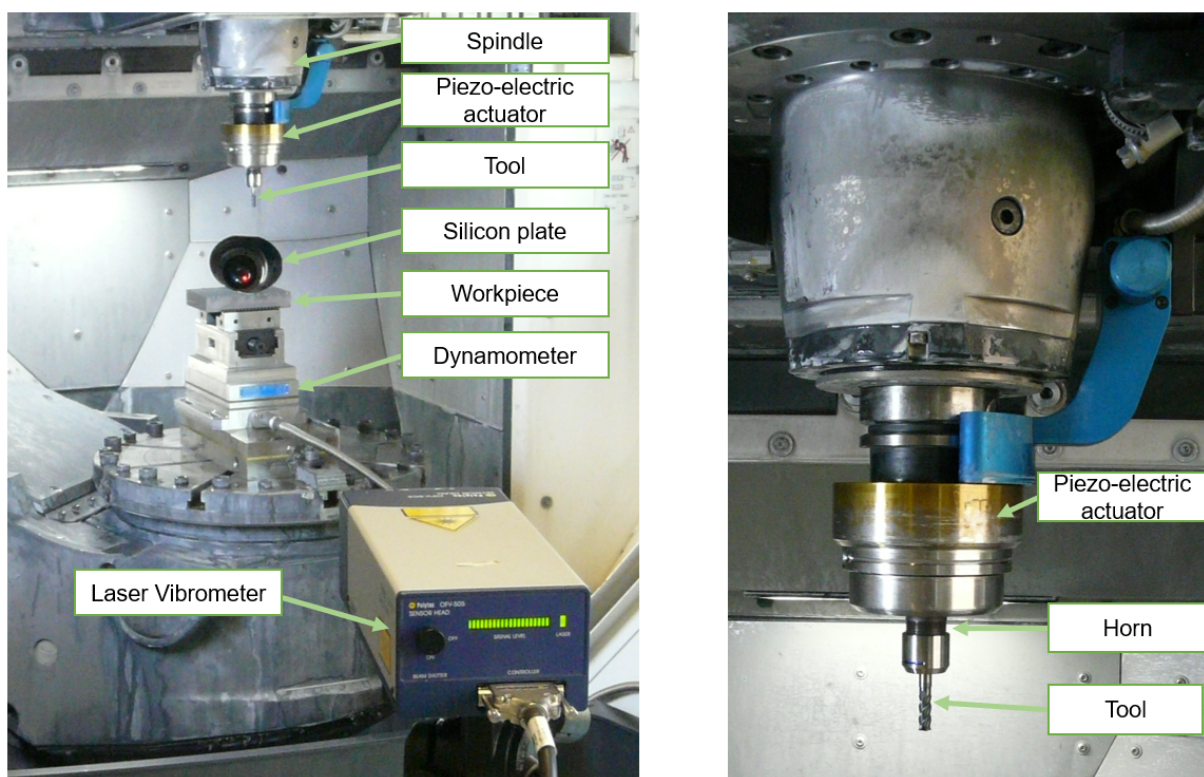


Figure 4-1: Longitudinal vibration measurement setup (left) and parts of the main spindle (right)

Longitudinal and torsional vibration amplitudes and frequencies were measured with a Polytec OFV-505 sensor head and Polytec OFV-5000 vibrometer controller. By using a silicon plate laser was reflected to the end cutting edge to measure longitudinal vibrations and by reflecting it directly to the tools rake face torsional vibrations were measured. However, torsional vibrations would not be considered during the experimental validation as the measured value was quite small and the helix angle of the tool could have caused errors during measurement.

The workpiece is a Ti-6Al-4V 25x80x12mm block mounted on the platform with clamping brackets. Detailed information about Ti-6Al-4V can be found on the Section 2.1.

A coated solid carbide tool of HPMT NiTiCo Line 30 was selected for both conventional and ultrasonic vibration assisted milling experiments. The selected 4 flute tool has a helix angle β of 40° and the mono layer AlCrN coating can stand temperatures up to 1100°C, the illustration of the tool can be seen in Figure 4-2 and more information about the tool dimensions is given in Table 4-1

Table 4-1: Tool dimensions

| | |
|--|-------|
| Diameter (D) | 6 mm |
| Length of Cut (l_1) | 16 mm |
| Length Below Shank (l_2) | 20 mm |
| Overall Length (L) | 50 mm |
| Rake Angle (γ) | 10° |

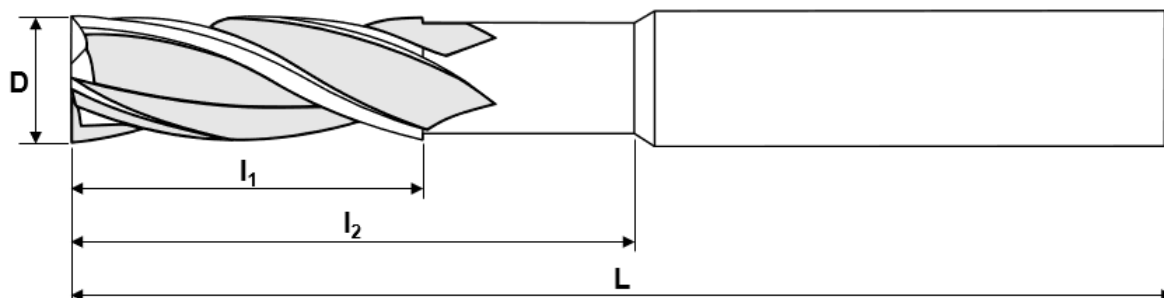


Figure 4-2: Illustration of HPTM solid carbide tool

Ultrasonic vibrations are generated by the piezo-electric actuators in a coaxial direction to the tool and are amplified by the horn before reaching to the carbide tool. Torsional vibrations are generated by the longitudinal vibrations. As the tool oscillates vertical to the workpiece the helix angle and the elasticity of the carbide tool causes the tool to periodically rotate bidirectionally.

4.2 Tool Wear Experiments

Four sets of experiments were conducted with 4 new tools to validate the tool life models and understand the effects of ultrasonic vibrations on tool wear. 2 sets of the experiments were done with conventional and the other 2 sets were done with ultrasonic vibration assisted milling. Same milling parameters were chosen to understand the effects of ultrasonic vibration assisted milling on tool wear. After milling 1,44 meters with each tool, tools were detached and investigated for tool wear under a microscope.

Slotting experiments were conducted and 346 cm^2 of Ti-6Al-4V was milled for each tool. During experiments the piezoelectric actuators get warmer, they began to work in lower amplitudes. In the following Table 4-2 machining parameters are given. UVAM stands for ultrasonic vibration and CM stands for conventional milling.

Table 4-2: Experimental conditions for tool life testing

| Experiment Number | Vibration Frequency (f_{os}) in kHz | Longitudinal Vibration Amplitude (A_l) in μm | Axial Depth of Cut (a_p) in mm | Feed per Tooth (f_z) in mm/T | Cutting Speed (v_c) in m/min |
|-------------------|---|---|------------------------------------|---|---|
| CM_01 | 0 | 0 | 0,4 | 0,06 | 40 |
| CM_02 | 0 | 0 | 0,4 | 0,06 | 90 |
| UVAM_01 | 22,6-22,75 | 2,2-2,7 | 0,4 | 0,06 | 40 |
| UVAM_02 | 22,6-22,75 | 2,2-2,7 | 0,4 | 0,06 | 90 |

Achieved ultrasonic vibration speed in cutting direction can be calculated by Equation 3-23. The achieved vibration speed in cutting direction, in vibration assisted milling experiments is 17,74 m/min, which is lower than both cutting speeds. Therefore, during the experiments no separation between tools rake face and workpiece happened due to low amplitude ultrasonic vibrations.

However, cutting edge of the carbide tool periodically exit and enter workpiece material because of the longitudinal vibrations. This hammering effect can cause work hardening of the material and if the depth of cut is not thicker than the work hardened layer it might result in higher wear rates. In the conducted experiments the workpiece was slotted with the carbide tool, then to begin working with a new surface, slotted surface was face milled with another tool without any ultrasonic vibration assistance. This generates a new, not work hardened surface to begin the next slotting experiment.

In experiments strong adhesion of Ti-6Al-4V on carbide tool was observed in both conventional and ultrasonic vibration assisted milling of Ti-6Al-4V. Adhered titanium and the built up edge makes it quite hard to measure the wear lands especially on tool tip. Two pictures of a new carbide tool can be seen in Figure 4-3.

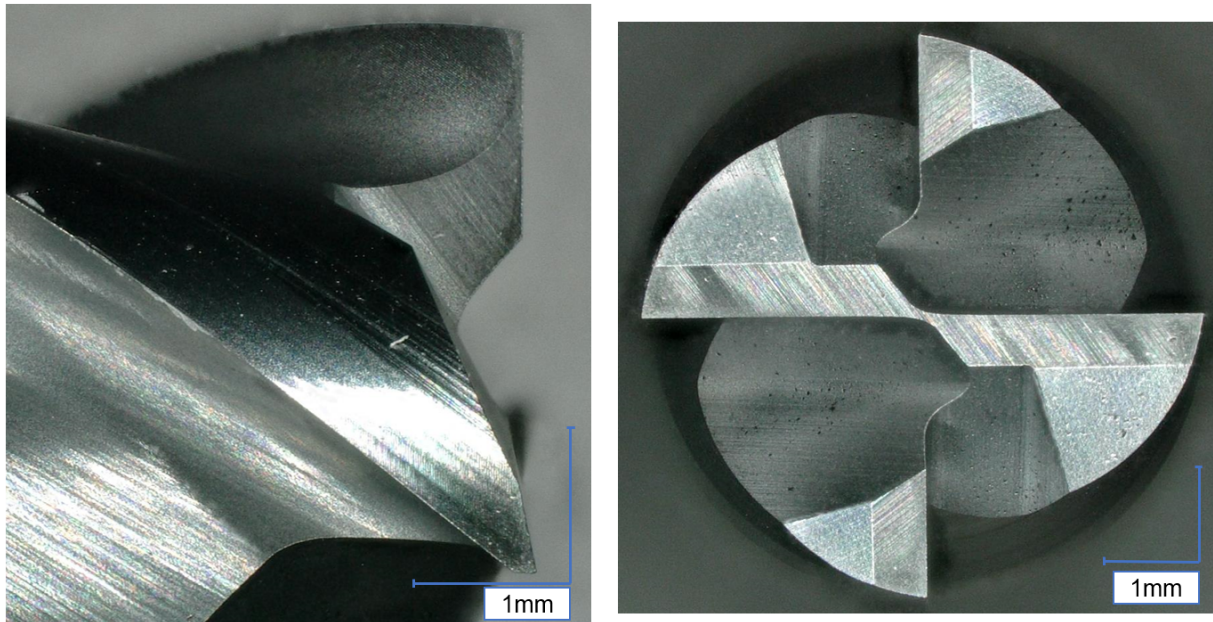


Figure 4-3: New carbide tool side view (left) and top view (right)

As seen in Figure 4-3 new tool has sharp edges and a uniform color. However after milling, strong adhesions can be seen on both tools used in conventional and vibration assisted milling. In Figure 4-4 end cutting edges of tools can be seen after milling 14,4 meters with a cutting speed of 90 meters per minute. Exact milling parameters can be seen in Table 4-2.

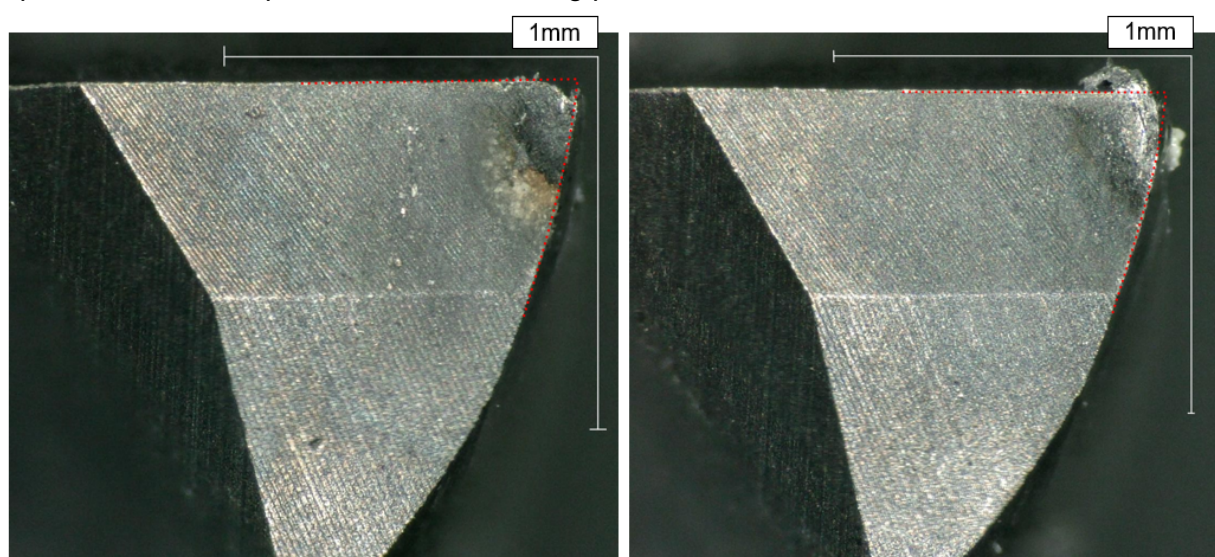


Figure 4-4: End cutting edge of 1st flute of the tool after 14,4 m of conventional milling (left) and ultrasonic vibration assisted milling (right)

Red points in the Figure 4-4 illustrate the undeformed tool tip and flank wear is visible on both tool end cutting edges. However, measurement of the wear land is not possible because of the adhered Titanium. Excessive adhesion is especially visible on ultrasonic vibration assisted milling as seen in Figure 4-4. However, this was just the case in this figure, excessive adhesion was also seen in conventional milling of Ti-6Al-4V. No significant wear difference was seen on the end cutting edge between ultrasonic vibration assisted and conventional milling.

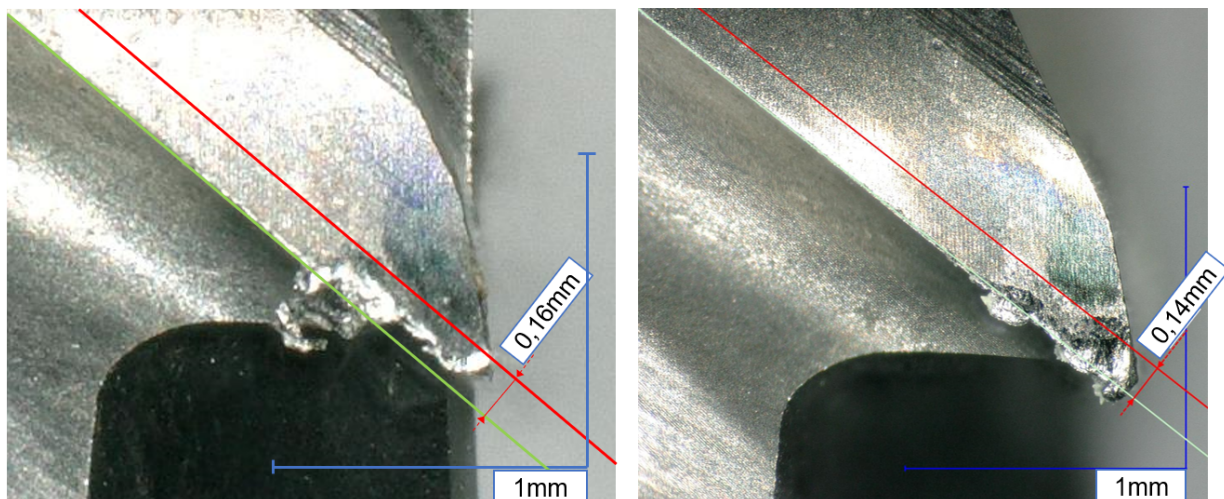


Figure 4-5: Relief flank wear on the 4th flute after 12,6 minutes (14,4 m) of conventional milling (left) and ultrasonic vibration assisted milling (right)

Figure 4-5 shows relief flank wear of 4th flute of the carbide tools after milling 14,4 meters with a cutting speed of 90m/min. Exact milling parameters can be seen in Table 4-2. As seen in the both microscope pictures adhesion is a dominant wear mechanism when milling Ti-6Al-4V. In this figure less flank wear is seen on the tool used in ultrasonic vibration assisted milling. Chipping of the peripheral cutting edge can be seen on the tool used in conventional milling however no chipping was observed in vibration assisted milling.

In the previous chapter we mentioned that more flank wear on the peripheral cutting edge can be expected during ultrasonic vibration assisted milling. The reason was the extra movement caused by the ultrasonic vibrations. However reduced cutting forces are also a well-known benefit of ultrasonic vibration assisted milling. As seen in Figure 4-5 reduced flank wear can be seen on the peripheral cutting edge of the carbide tool.

According to LITTMANN ET AL. (2002), friction forces can be reduced significantly during machining, when high frequency ultrasonic vibrations are superimposed on the conventional movement of the cutting tool. This force reduction without any tool and workpiece separation can cause less flank wear on the peripheral cutting edge. However BIGELMAIER (2017) observed up to 12,7% cutting force reduction during vibration assisted milling without any tool rake face and workpiece separation.

Contradictory results were found by researchers when face milling hard to machine nickel alloy 718 with longitudinal vibration assisted milling without any tool flank face and workpiece separation. SUÁREZ ET AL. (2016) observed 10% more flank wear than conventional milling when using ultrasonic vibration assistance. However, SUÁREZ ET AL. (2016) used almost half the amplitude and almost two times the vibration frequency of the amplitude and vibration frequency that were used on our experiments. This would than give approximately the same vibration speed on both conducted experiments however, the tool wear results still vary.

Conflicting results can be explained by different tool-workpiece combinations, which can cause different tool wear patterns due to ultrasonic vibrations. SUÁREZ ET AL. (2016) only observed a slight reduction of the passive forces when ultrasonic vibrations were introduced. However BIGELMAIER (2017) observed up to 12,7% cutting force reduction during vibration assisted milling without any tool rake face and workpiece separation.

Experiments conducted with a cutting speed of 40 m/min didn't show any significant tool wear after 14.4 meters (28 minutes) as seen in Figure 4-6, it is not possible to measure the amount of wear because of the adhered titanium on the wear land and the built up edge.

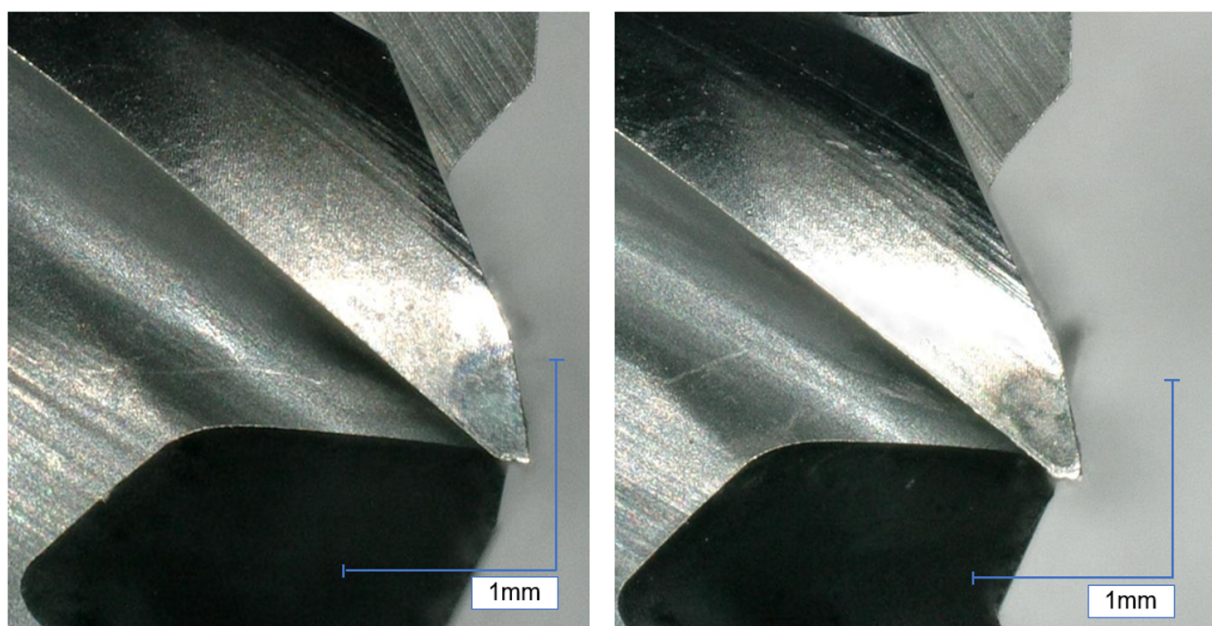


Figure 4-6: Relief side of the 3rd flute after 28 minutes (14,4m) of conventional milling (left)
and ultrasonic vibration assisted milling (right)

As the wear land is not visible in Figure 4-6, only the results of the conventional and ultrasonic vibration assisted milling experiments with a cutting speed of 90 m/min can be used for validation.

Amount of tool life tests done in this thesis is not enough to determine the tool and workpiece specific constants. In Equation 3-36, four tool and workpiece specific constants can be seen, determining four constants with two experiments wouldn't result with accurate constants.

However the constant γ in Equation 3-36 can be determined by making a comparison between the wear lands of tools used in conventional and ultrasonic vibration assisted milling. Ultrasonic vibration assisted milling did cause a 13% decrease in tool wear. Assuming that this 13% decrease would result in a 13% increase in tool life the constant γ can be calculated with the following Equation 4-1.

$$\left(\frac{v_c + v_{UV,co}}{v_c} \right)^\gamma \approx 1.13 \quad (4-1)$$

Where cutting speed v_c is 90 m/min and the combined ultrasonic vibration speed (in this situation only the longitudinal vibration speed) $v_{UV,co}$ is 17,74 m/min. Logarithms taken on both sides of Equation 4-1 transforms the equation into a linear estimation problem as seen in Equation 4-2. By using the mentioned values the approximate value of constant γ can be calculated.

$$\gamma \cdot \ln \left(\frac{v_c + v_{UV,co}}{v_c} \right) = \ln 1.13 \quad (4-2)$$

So the approximate value of γ is 0.68. By using this value an approximate tool life on ultrasonic vibration assisted milling can be found.

5 Summary and Future Work

In the presented bachelors thesis, a new tool wear model for ultrasonic vibration assisted milling has been developed. The model is able to determine tool life in ultrasonic vibration assisted milling in the phases with and without periodic tool-workpiece separation.

In the beginning, in order to have a better understanding of the workpiece material, mechanical and chemical properties of Ti-6Al-4V have been investigated. Then the main differences between conventional milling and ultrasonic vibration assisted milling was explained and the effects of ultrasonic vibrations on tool wear was studied.

In order to develop a new wear model, dominant tool wear mechanisms in titanium milling were researched and the appearance of different wear mechanisms on cutting tool were investigated. In course of developing a new tool wear model, existing tool wear models for conventional milling were researched and the assumptions, that the models are based on were discussed.

Yellowley and Barrow's tool life model was chosen for further development for describing the tool life in ultrasonic vibration assisted milling. In order to describe the effects of milling parameters on tool wear, a new milling parameter "Maximum equivalent chip thickness" was introduced. With the aim of determining the maximum equivalent chip thickness, first the maximum undeformed chip thickness on a face milling operation was calculated and by using the assumptions of Woxén the maximum equivalent chip thickness was determined.

In order to create a new wear model, that would be able to describe the effects of ultrasonic vibrations, two different tool life equations were developed for two different cases. The first equation was developed to model the tool life with a periodic tool-workpiece separation due to the ultrasonic vibrations. The contact ratio of tool and workpiece was calculated to describe the tool life enchanting effects of ultrasonic vibrations. The tool wear model was based on the assumption, that there would be a proportionality between the contact ratio and the tool life. The second equation was developed to model the tool life without any tool rake face and workpiece separation. In order to model this phase the resulting vibration speed is calculated and used for building a ratio between the cutting speed and ultrasonic vibration speed. It was assumed that the tool life would be proportional to the calculated ratio.

Fehler! Verwenden Sie die Registerkarte 'Start', um Heading 1 dem Text zuzuweisen,
der hier angezeigt werden soll.

Contradictory reports were found in literature about tool wear in ultrasonic vibration assisted milling without tool-workpiece separation. Conducted experiments showed that ultrasonic vibration assisted milling has caused 13% less wear than conventional milling. By using the experimental data a constant of the presented tool life model was calculated.

Presented tool life models can be used in different tool- workpiece material combinations, once the material specific constants were determined. However, titanium is a hard to machine material and it is possible that when using a different tool-workpiece combination ultrasonic vibrations might have different effects on tool wear.

Future work can be done by performing a temperature and wear simulation of the tool to understand the effects of ultrasonic vibrations on tool wear. Temperature and stress based tool life equations can be further developed to determine a different approach on tool wear in vibration assisted milling. The developed contact ratio model doesn't consider the springback effect of the machined surface, considering this effect would cause higher contact ratios and therefore, effect the results of the developed tool life equations.

6 Bibliography

ALTINTAS 2011

Altintas, Y.: Manufacturing Automation. Cambridge: Cambridge University Press 2011. ISBN: 9780511843723.

ARCHARD 1953

Archard, J. F.: Contact and Rubbing of Flat Surfaces. Journal of Applied Physics 24 (1953) 8, p. 981-988.

AZO MATERIALS 2002

Azo Materials: Titanium Alloys - Ti6Al4V Grade 5.
<<https://www.azom.com/article.aspx?ArticleID=1547>> - 09.04.2018.

BABITSKY ET AL. 2003

Babitsky, V.I.; Kalashnikov, A.N.; Meadows, A.; Wijesundara, A.A.H.P.: Ultrasonically assisted turning of aviation materials. Journal of Materials Processing Technology 132 (2003) 1-3, p. 157-167.

BARGEL ET AL. 2008

Bargel, H.-J.; Hilbrans, H.; Schulze, G.: Werkstoffkunde. 10., bearb. Aufl. Aufl. Berlin: Springer 2008. ISBN: 978-3-540-79296-3. (VDI-Buch).

BARROW 1972

Barrow, G.: Tool-Life Equations and Machining Economics. In: Koenigsberger, F. et al. (Hrsg.): Proceedings of the Twelfth International Machine Tool Design and Research Conference. London: Macmillan Education UK 1972, p. 481-493. ISBN: 978-1-349-01399-9.

BIGELMAIER 2017

Bigelmaier, M.: Implementierung eines Zerspankraftmodells für das schwingungsunterstützte Fräsen (Master's dissertation) Institute for Machine Tools and Industrial Management Technical University of Munich. Munich (01/06/2017).

Fehler! Verwenden Sie die Registerkarte 'Start', um Heading 1 dem Text zuzuweisen,
der hier angezeigt werden soll.

BREHL & DOW 2008

Brehl, D. E.; Dow, T. A.: Review of vibration-assisted machining. *Precision Engineering* 32 (2008) 3, p. 153-172.

BUDAK & KOPS 2000

Budak, E.; Kops, L.: Improving Productivity and Part Quality in Milling of Titanium Based Impellers by Chatter Suppression and Force Control. *CIRP Annals* 49 (2000) 1, p. 31-36.

BURWELL & STRANG 1952

Burwell, J. T.; Strang, C. D.: On the Empirical Law of Adhesive Wear. *Journal of Applied Physics* 23 (1952) 1, p. 18-28.

CHE-HARON 2001

Che-Haron, C.H.: Tool life and surface integrity in turning titanium alloy. *Journal of Materials Processing Technology* 118 (2001) 1-3, p. 231-237.

COLDING 1961

Colding, B. N.: Machinability of metals and machining costs. *International Journal of Machine Tool Design and Research* 1 (1961) 3, p. 220-248.

COLDING 1991

Colding, B. N.: A Tool-Temperature/Tool-Life Relationship Covering a Wide Range of Cutting Data. *CIRP Annals* 40 (1991) 1, p. 35-40.

CONG & PEI 2013

Cong, W.; Pei, Z.: Process of Ultrasonic Machining. In: Nee, A. (Hrsg.): *Handbook of Manufacturing Engineering and Technology*. London: Springer London 2013, p. 1-19. ISBN: 978-1-4471-4976-7.

CORDUAN ET AL. 2003

Corduan, N.; Himbart, T.; Poulachon, G.; Dessoly, M.; Lambertin, M.; Vigneau, J.; Payoux, B.: Wear Mechanisms of New Tool Materials for Ti-6Al-4V High Performance Machining. CIRP Annals 52 (2003) 1, p. 73-76.

CRANK 1979

Crank, J.: The mathematics of diffusion. 2nd ed. Aufl. Oxford: Clarendon Press 1979. ISBN: 9780198534112. (Oxford science publications).

DADIC 2013

Dadic, Z. (Hrsg.): Tribological principles and measures to reduce cutting tools wear. Split, Croatia, 26-27.09.2013. 2013.

DEARNLEY & GREARSON 2013

Dearnley, P. A.; Gearson, A. N.: Evaluation of principal wear mechanisms of cemented carbides and ceramics used for machining titanium alloy IMI 318. Materials Science and Technology 2 (2013) 1, p. 47-58.

DEPIERREUX 1969

Depiereux, W. R.: Die Ermittlung optimaler Schnittbedingungen, insbesondere, im Hinblick auf die wirtschaftliche Nutzung numerisch gesteuerter Werkzeugmaschinen (Ph.D. Thesis) Technische Hochschule Aachen. Aachen (1969).

DOLINŠEK & KOPAČ 2006

Dolinšek, S.; Kopač, J.: Mechanism and types of tool wear; particularities in advanced cutting materials. , Journal of Achievement in Materials and Manufacturing Engineering 19 (2006), p. 1-8.

EZUGWU & WANG 1997

Ezugwu, E. O.; Wang, Z. M.: Titanium alloys and their machinability—a review. Journal of Materials Processing Technology 68 (1997) 3, p. 262-274.

EZUGWU ET AL. 2003

Ezugwu, E.O.; Bonney, J.; Yamane, Y.: An overview of the machinability of aeroengine alloys. *Journal of Materials Processing Technology* 134 (2003) 2, p. 233-253.

GU ET AL. 1999

Gu, J.; Barber, G.; Tung, S.; Gu, R.-J.: Tool life and wear mechanism of uncoated and coated milling inserts. *Wear* 225-229 (1999), p. 273-284.

HARTUNG ET AL. 1982

Hartung, P. D.; Kramer, B. M.; Turkovich, B. F. von: *Tool Wear in Titanium Machining*. CIRP Annals 31 (1982) 1, p. 75-80.

HEISEL ET AL. 2014

Heisel, U.; Stehle, T.; Eisseler, R.; Eber, R.; Jakob P.: Schwingungsunterstütztes Fräsen von Formnuten in 42CrMo4. wt *Werkstattstechnik online* (2014), p. 22-26.

HOLM 1946

Holm, R.: *Electric Contacts*. Stockholm: Hugo Gebers Förlag 1946.

HOLM 1967

Holm, R.: *Electric Contacts*. Berlin, Heidelberg: Springer Berlin Heidelberg 1967. ISBN: 978-3-642-05708-3.

HOSSEINI & KISHAWY 2014

Hosseini, A.; Kishawy, H. A.: Cutting Tool Materials and Tool Wear. In: Davim, J. P. (Hrsg.): *Machining of titanium alloys*. New York: Springer 2014, p. 31-56. ISBN: 978-3-662-43901-2.

ISO 3685:1993

ISO 3685:1993: Tool-life testing with single-point turning tools: 11.1993.

JANGHORBANIAN ET AL. 2013

Janghorbanian, J.; Razfar, M. R.; Abootorabi Zarchi, M. M.: Effect of cutting speed on tool life in ultrasonic-assisted milling process. Proceedings of the Institution of Mechanical Engineers, Part B: Journal of Engineering Manufacture 227 (2013) 8, p. 1157-1164.

JAWAID ET AL. 2000

Jawaid, A.; Sharif, S.; Koksal, S.: Evaluation of wear mechanisms of coated carbide tools when face milling titanium alloy. Journal of Materials Processing Technology 99 (2000) 1-3, p. 266-274.

JOHANSSON ET AL. 2017

Johansson, D.; Hägglund, S.; Bushlya, V.; Ståhl, J.-E.: Assessment of Commonly used Tool Life Models in Metal Cutting. Procedia Manufacturing 11 (2017), p. 602-609.

KÖNIG ET AL. 1991

König, W.; Fritsch, R.; Kammermeier, D.: Physically vapor deposited coatings on tools. Surface and Coatings Technology 49 (1991) 1-3, p. 316-324.

KUMAR ET AL. 2014

Kumar, M. N.; Subbu, S. K.; Krishna, P. V.; Venugopal, A.: Vibration Assisted Conventional and Advanced Machining. Procedia Engineering 97 (2014), p. 1577-1586.

LI ET AL. 2012

Li, C. P.; Kim, M. Y.; Ko, T. J.; Park, J. K.: The effects of ultrasonic vibration on surface finish and tool wear in end-milling machining. In: Eichhorn, V. (Hrsg.): 2012 International Conference on Manipulation, Manufacturing and Measurement on the Nanoscale (3M-NANO 2012). Xi'an, China. Piscataway, NJ, Piscataway, NJ: IEEE 2012, p. 330-334. ISBN: 978-1-4673-4590-3.

LITTMANN ET AL. 2002

Littmann, W.; Storck, H.; Wallaschek, J.: Reibung bei Ultraschallschwingungen VDI-Gesellschaft Entwicklung Konstruktion Vertrieb 2002. ISBN: 3180917369.

MACHADO & WALLBANK 2016

Machado, A. R.; Wallbank, J.: Machining of Titanium and its Alloys—a Review. Proceedings of the Institution of Mechanical Engineers, Part B: Journal of Engineering Manufacture 204 (2016) 1, p. 53-60.

MIN & YOZHENG 2013

Min, W.; Youzhen, Z.: Diffusion wear in milling titanium alloys. Materials Science and Technology 4 (2013) 6, p. 548-553.

MÜLLER 1982

Müller, M.: Zerspankraft, Werkzeugbeanspruchung und Verschleiß beim Fräsen mit Hartmetall. Berlin, Heidelberg: Springer Berlin Heidelberg 1982. ISBN: 978-3-540-11506-9. (WBK-Forschungsberichte aus dem Institut für Werkzeugmaschinen und Betriebstechnik der Universität Karlsruhe 6).

NABHANI 2001

Nabhani, F.: Wear mechanisms of ultra-hard cutting tools materials. Journal of Materials Processing Technology 115 (2001) 3, p. 402-412.

NATEGH ET AL. 2009

Nategh, M. J.; Amini, S.; Soleimanimehr, H.: Modeling the Force, Surface Roughness and Cutting Temperature in Ultrasonic Vibration-Assisted Turning of Al7075. Advanced Materials Research 83-86 (2009), p. 315-325.

NATH & RAHMAN 2008

Nath, C.; Rahman, M.: Effect of machining parameters in ultrasonic vibration cutting. International Journal of Machine Tools and Manufacture 48 (2008) 9, p. 965-974.

NEE 2013

Nee, Andrew (Hrsg.): Handbook of Manufacturing Engineering and Technology. London: Springer London 2013. ISBN: 978-1-4471-4976-7.

NOUARI & GINTING 2006

Nouari, M.; Ginting, A.: Wear characteristics and performance of multi-layer CVD-coated alloyed carbide tool in dry end milling of titanium alloy. *Surface and Coatings Technology* 200 (2006) 18-19, p. 5663-5676.

OOSTHUIZEN 2010

Oosthuizen, G. A.: Wear characterisation in milling of Ti6Al4V Stellenbosch : University of Stellenbosch (2010).
[<http://scholar.sun.ac.za/bitstream/10019.1/5426/1/oosthuizen_wear_2010.pdf>](http://scholar.sun.ac.za/bitstream/10019.1/5426/1/oosthuizen_wear_2010.pdf).

OXLEY 2007

Oxley, P. L.: DEVELOPMENT AND APPLICATION OF A PREDICTIVE MACHINING THEORY. *Machining Science and Technology* 2 (2007) 2, p. 165-189.

PATIL ET AL. 2014

Patil, S.; Joshi, S.; Tewari, A.; Joshi, S. S.: Modelling and simulation of effect of ultrasonic vibrations on machining of Ti6Al4V. *Ultrasonics* 54 (2014) 2, p. 694-705.

PEKELHARING 1984

Pekelharing, A. J.: The Exit Failure of Cemented Carbide Face Milling Cutters Part I — Fundamentals and Phenomenae. *CIRP Annals* 33 (1984) 1, p. 47-50.

PRAMANIK & LITTLEFAIR 2015

Pramanik, A.; Littlefair, G.: Machining of Titanium Alloy (Ti-6Al-4V) —Theory to Application. *Machining Science and Technology* 19 (2015) 1, p. 1-49.

PUJANA ET AL. 2009

Pujana, J.; Rivero, A.; Celaya, A.; López de Lacalle, L. N.: Analysis of ultrasonic-assisted drilling of Ti6Al4V. *International Journal of Machine Tools and Manufacture* 49 (2009) 6, p. 500-508.

QUINTANA & CIURANA 2011

Quintana, G.; Ciurana, J.: Chatter in machining processes. *International Journal of Machine Tools and Manufacture* 51 (2011) 5, p. 363-376.

SADIK ET AL. 2016

Sadik, M. I.; Isakson, S.; Malakizadi, A.; Nyborg, L.: Influence of Coolant Flow Rate on Tool Life and Wear Development in Cryogenic and Wet Milling of Ti-6Al-4V. Procedia CIRP 46 (2016), p. 91-94.

STEPHENSON & AGAPIOU 2016

Stephenson, D. A.; Agapiou, J. S.: Metal Cutting Theory and Practice. Third Edition Aufl. 2016. ISBN: 1466587547.

SU ET AL. 2006

Su, Y.; He, N.; Li, L.; Li, X. L.: An experimental investigation of effects of cooling/lubrication conditions on tool wear in high-speed end milling of Ti-6Al-4V. Wear 261 (2006) 7-8, p. 760-766.

SUÁREZ ET AL. 2016

Suárez, A.; Veiga, F.; Lacalle, L. N. de; Polvorosa, R.; Lutze, S.; Wretland, A.: Effects of Ultrasonics-Assisted Face Milling on Surface Integrity and Fatigue Life of Ni-Alloy 718. Journal of Materials Engineering and Performance 25 (2016) 11, p. 5076-5086.

SUPRA ALLOYS 2018

Supra Alloys: Titanium Grades Information - Properties and Applications for all Titanium Alloys & Pure Grades. <<http://www.supralloys.com/titanium-grades.php>> - 4/9/2018.

TAKEYAMA & MURATA 1963

Takeyama, H.; Murata, R.: Basic Investigation of Tool Wear. Journal of Engineering for Industry 85 (1963) 1, p. 33.

TAYLOR 1907

Taylor, F. W.: On the art of cutting metals (An adress made at the opening of the annual meeting in New York 1906). 3 Aufl. 1907: The American Society of Mechanical Engineers 1907.

Fehler! Verwenden Sie die Registerkarte 'Start', um Heading 1 dem Text zuzuweisen,
der hier angezeigt werden soll.

TRIGGER & CHAO 1956

Trigger, K. J.; Chao, B. T.: The Mechanism of Crater Wear of Cemented Carbide Tools.
Transactions of the American Society of Mechanical Engineers 78 (1956).

TSAI ET AL. 2016

Tsai, M.; Chang, C.; Ho, J.: The Machining of Hard Mold Steel by Ultrasonic Assisted End Milling. Applied Sciences 6 (2016) 11, p. 373.

UHLIG 2018

Uhlig, L.-M.: Valbruna Werkstoffdatenblatt Ti-6Al-4V.
<<https://www.valbruna.de/files/pdf/datenblatt-3.7164-3.7165.pdf>> - 4/9/2018.

USUI ET AL. 1978

Usui, E.; Shirakashi, T.; Kitagawa, T.: Analytical Prediction of Three Dimensional Cutting Process—Part 3. Journal of Engineering for Industry 100 (1978) 2, p. 236.

WAN ET AL. 2017

Wan, M.; Feng, J.; Zhang, W.-H.; Yang, Y.; Ma, Y.-C.: Working mechanism of helix angle on peak cutting forces together with its design theory for peripheral milling tools. Journal of Materials Processing Technology 249 (2017), p. 570-580.

WOLDMAN & GIBBONS 1951

Woldman, N. E.; Gibbons, R. C.: Machinability and Machining of Metals. New York: McGraw-Hill Book Company 1951.

WOXÉN 1932

Woxén, R.: A theory and an equation for the life of lathe tools. Stockholm: Centraltryckeriet 1932. (Avhandling Tekniske högskolan 10).

YELLOWLEY & BARROW 1971

Yellowley, I.; Barrow, G.: Ermittlung und Anwendung von Bearbeitbarkeitsangaben. Fertigung 1 (1971), p. 21-29.

Fehler! Verwenden Sie die Registerkarte 'Start', um Heading 1 dem Text zuzuweisen,
der hier angezeigt werden soll.

ZANGER 2013

Zanger, F.: Segmentspanbildung, Werkzeugverschleiß, Randschichtzustand und Bauteileigenschaften. Numerische Analysen zur Optimierung des Zerspanungsprozesses am Beispiel von Ti-6Al-4V (Zugl.: Karlsruhe, Inst. für Technologie, Diss., 2012). Aachen: Shaker 2013. ISBN: 9783844016451. (Forschungsberichte aus dem wbk, Institut für Produktionstechnik Universität Karlsruhe 169).

ZHANG ET AL. 2017

Zhang, Y.; Zhao, B.; Wang, Y.; Chen, F.: Effect of machining parameters on the stability of separated and unseparated ultrasonic vibration of feed direction assisted milling. Journal of Mechanical Science and Technology 31 (2017) 2, p. 851-858.

ZOYA & KRISHNAMURTHY 2000

Zoya, Z.A.; Krishnamurthy, R.: The performance of CBN tools in the machining of titanium alloys. Journal of Materials Processing Technology 100 (2000) 1-3, p. 80-86.

Fehler! Verwenden Sie die Registerkarte 'Start', um Heading 1 dem Text zuzuweisen,
der hier angezeigt werden soll.

7 Content of the CD

0 - Digital version of this work

1 - Digital sources

2 - Figures

3 - Tool wear pictures

Fehler! Verwenden Sie die Registerkarte 'Start', um Heading 1 dem Text zuzuweisen,
der hier angezeigt werden soll.

8 Statutory Declaration

I declare that I have authored this thesis independently, that I have not used other than the declared sources / resources, and that I have explicitly marked all material which has been quoted either literally or by content from the used sources.

This thesis was not submitted in the same or in a substantially similar version, not even partially, to any other authority to achieve an academic grading and was not published elsewhere.

Munich, 15.05.2018

Alpcan Güray

Acknowledgement
